Report #04034

RESOLVE SURVEY
FOR
U. S. GEOLOGICAL SURVEY

EAST POPLAR OIL FIELDS, MONTANA

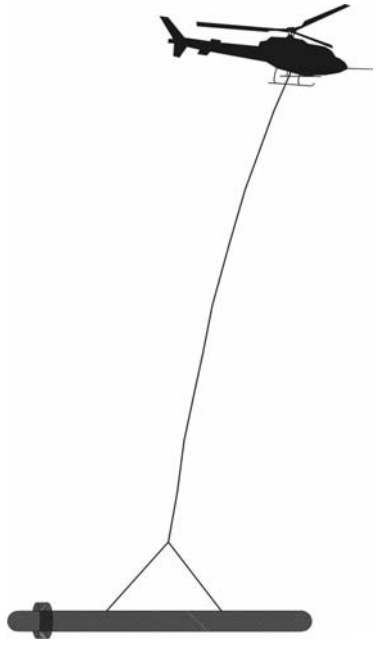

Fugro Airborne Surveys Corp.
Mississauga, Ontario

Michael J. Cain
Geophysicist

October 2004

SUMMARY

This report describes the logistics, data acquisition and processing of a RESOLVE airborne geophysical survey carried out for the U. S. Geological Survey, over parts of the East Poplar Oil Fields, Montana. Total coverage of the survey blocks amounted to 1645 kms. The survey was flown from August 12th to 14th, 2004.

The purpose of the survey was to map the conductive and magnetic properties of the survey area. This was accomplished by using a RESOLVE multi-coil, multi-frequency electromagnetic system, supplemented by a high sensitivity cesium magnetometer. The information from these sensors was processed to produce maps that display the magnetic and conductive properties of the survey area. A GPS electronic navigation system ensured accurate positioning of the geophysical data with respect to the base maps.

The survey data were processed and compiled in the Fugro Airborne Surveys office. Map products and digital data were provided in accordance with the scales and formats specified in the Survey Agreement.

CONTENTS

APPENDICES

A. List of Personnel
B. Data Archive Description
C. Background Information
D. Flight Logs
E. Tests and Calibrations
F. Processing Log
G. Glossary

1. INTRODUCTION

A RESOLVE electromagnetic/resistivity/magnetic survey was flown for the U. S. Geological Survey from August 12th to 14th, 2004, over part of the East Poplar Oil Fields, Montana.

Survey coverage consisted of 1645 line-km, over 1 block, including two detail areas. Flight lines were flown in an azimuthal direction of 0°/180° with a line separation of 200 metres. The detail areas were flown within the main survey area with an offset of 100 metres, giving an effective line spacing of 100 metres. Two tie lines were flown perpendicular to the survey lines.

The survey employed the RESOLVE electromagnetic system. Ancillary equipment consisted of a high sensitivity cesium magnetometer, radar, laser and barometric altimeters, video camera, analog and digital recorders, and an electronic navigation system. The instrumentation was installed in an AS350-B3 turbine helicopter (Registration C-GECL) that was provided by Questral Helicopters Ltd. The helicopter flew at an average airspeed of 125 km/h with an EM sensor height of approximately 33 metres.

Figure 1: Fugro Airborne Surveys RESOLVE EM bird with AS350-B3 helicopter, at Wolf Point, Montana, airport. USGS project chief, Johanna Thamke, is standing at the forward end of the 10 meter long “bird” which houses the geophysical systems (electromagnetic, magnetic, and laser altimeter).

2. SURVEY OPERATIONS

The base of operations for the survey was established in Wolf Point, Montana. The helicopter was based and fueled out of the Wolf Point airport. The base stations were established and operated on the airport grounds.

Table 2.1 - Survey Specifications

Parameter	Specifications
Traverse line direction	0°/180°
Traverse line spacing	200 m
Tie line direction	90°/270°
Tie line spacing	7000 m
Sample interval	10 Hz or 3.5 m at 125 km/hr
Aircraft mean terrain clearance	60 m
EM sensor mean terrain clearance	33 m
Mag sensor mean terrain clearance	33 m
Average speed	125 km/hr
Navigation (guidance)	±5 m, Real-time GPS
Post-survey flight path	±2 m, Differential GPS

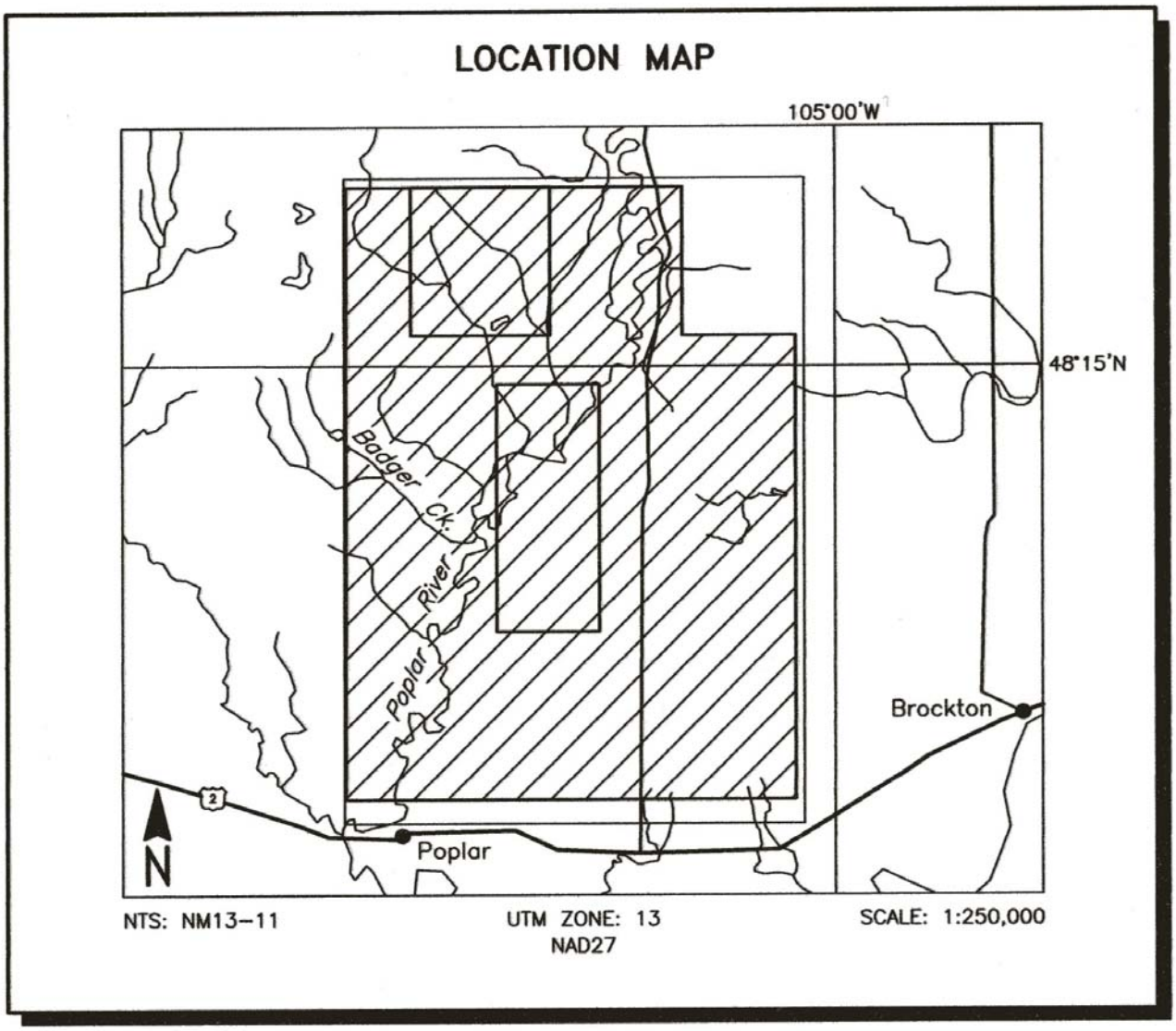

Figure 2
Location Map and Sheet Layout
East Poplar Oil Fields, Montana
Job # 04034

Table 2.2 – Survey Block Corners

Main Survey Area

NAD27 UTM Zone 13

Block	Corners	X-UTM (E)	Y-UTM (N)
04034-1	1	484062	5349715
East Poplar	2	495017	5349714
Oil Fields	3	495017	5344884
	4	498713	5344884
	5	498713	5329783
	6	484036	5329784

Detail Blocks

NAD27 UTM Zone 13

Block	Corners	X-UTM (E)	Y-UTM (N)
04034-2	1	486171	5349720
East Poplar	2	490706	5349720
Oil Fields	3	490706	5344898
	4	486171	5344898
04034-3	1	488962	5343282
East Poplar	2	492309	5343282
Oil Fields	3	492309	5335240
	4	488962	5335240

3. SURVEY EQUIPMENT

This section provides a brief description of the geophysical instruments used to acquire the survey data and the calibration procedures employed. The geophysical equipment was installed in an AS350-B3 helicopter. This aircraft provides a safe and efficient platform for surveys of this type.

Electromagnetic System

Model: RESOLVE

Type: Towed bird, symmetric dipole configuration operated at a nominal survey altitude of 30 metres. Coil separation is 7.9 metres for 400 Hz, 1800 Hz, 8200 Hz, 40,000 Hz and 140,000 Hz coplanar coil-pairs; and 9.0 metres for the 3300 Hz coaxial coil-pair. The EM bird is towed on a cable measuring 28.7 metres (94 feet). Due to airlift and wind resistance on the bird and cable during flight, a slightly shorter value of 27.7 metres (91 feet) is subtracted from the radar altimeter data to give the approximate bird height. These results agree with the laser altimeter values at survey height and speed.

Coil orientations/frequencies:

orientation	nominal	actual
coplanar	400 Hz	391 Hz
coplanar	1800 Hz	1801 Hz
coaxial	3300 Hz	3326 Hz
coplanar	8200 Hz	8162 Hz
coplanar	40,000 Hz	39,130 Hz
coplanar	140,000 Hz	132,640 Hz

Channels recorded:
6 in-phase channels
6 quadrature channels
2 monitor channels

Sensitivity:	0.12 ppm at 400 Hz CP 0.12 ppm at 1800 Hz CP 0.12 ppm at 3300 Hz CX 0.24 ppm at 8200 Hz CP 0.60 ppm at 40,000 Hz CP 0.60 ppm at 140,000 Hz CP
Sample rate:	10 per second, equivalent to 1 sample every 3.5 m, at a survey speed of 125 km/h.

The electromagnetic system utilizes a multi-coil coaxial/coplanar technique to energize conductors in different directions. The coaxial coils are vertical with their axes in the flight direction. The coplanar coils are horizontal. The secondary fields are sensed simultaneously by means of receiver coils that are maximum coupled to their respective transmitter coils. The system yields an in-phase and a quadrature channel from each transmitter-receiver coil-pair.

RESOLVE System Calibration

Calibration of the system during the survey uses the Fugro AutoCal automatic, internal calibration process. At the beginning and end of each flight, and at intervals during the flight, the system is flown up to high altitude to remove it from any “ground effect” (response from the earth). Any remaining signal from the receiver coils (base level) is measured as the zero level, and removed from the data collected until the time of the next calibration. Following the zero level setting, internal calibration coils, for which the response phase and amplitude have been determined at the factory, are automatically triggered – one for each frequency. The on-time of the coils is sufficient to determine an accurate response through any ambient noise. The receiver response to each

calibration coil “event” is compared to the expected response (from the factory calibration) for both phase angle and amplitude, and the applied phase and gain corrections are adjusted to bring the data to the correct value. In addition, the output of the transmitter coils are continuously monitored during the survey, and the applied gains adjusted to correct for any change in transmitter output.

Because the internal calibration coils are calibrated at the factory (on a resistive halfspace) ground calibrations using external calibration coils on-site are not necessary for system calibration. A check calibration may be carried out on-site to ensure all systems are working correctly. All system calibrations will be carried out in the air, at sufficient altitude that there will be no measurable response from the ground.

The internal calibration coils are rigidly positioned and mounted in the system relative to the transmitter and receiver coils. In addition, when the internal calibration coils are calibrated at the factory, a rigid jig is employed to ensure accurate response from the external coils.

Using real time Fast Fourier Transforms and the calibration procedures outlined above, the data will be processed in real time from measured total field at a high sampling rate to in-phase and quadrature values at 10 samples per second.

Airborne Magnetometer

Model:	Fugro AM102 processor with Scintrex CS2 sensor
Type:	Optically pumped cesium vapour
Sensitivity:	0.01 nT
Sample rate:	10 per second

The magnetometer sensor is located inside the EM bird.

Magnetic Base Station

Primary

Model:	Fugro CF1 base station with timing provided by integrated GPS	
Sensor type:	Geometrics G822	
Counter specifications:	Accuracy:	±0.1 nT
	Resolution:	0.01 nT
	Sample rate	1 Hz
GPS specifications:	Model:	Marconi Allstar
	Type:	Code and carrier tracking of L1 band, 12-channel, C/A code at 1575.42 MHz
	Sensitivity:	-90 dBm, 1.0 second update
	Accuracy:	Manufacturer's stated accuracy for differential corrected GPS is 2 metres

Environmental Monitor specifications:

Temperature:

- Accuracy: ±1.5ºC max
- Resolution: 0.0305ºC
- Sample rate: 1 Hz
- Range: -40ºC to +75ºC

Barometric pressure:

- Model: Motorola MPXA4115A
- Accuracy: ±3.0º kPa max (-20ºC to 105ºC temp. ranges)
- Resolution: 0.013 kPa

- Sample rate: 1 Hz
- Range: 55 kPa to 108 kPa

Backup Magnetometer

Model:	GEM Systems GSM-19T
Type:	Digital recording proton precession
Sensitivity:	0.10 nT
Sample rate:	3 second intervals

A digital recorder is operated in conjunction with the base station magnetometer to record the diurnal variations of the earth's magnetic field. The clock of the base station is synchronized with that of the airborne system, using GPS time, to permit subsequent removal of diurnal drift. The CF1 base station was located at WGS84 latitude 48° 05.67532' N, longitude 105° 34.38384' W and 588.8 metres above the ellipsoid.

Navigation (Global Positioning System)

Airborne Receiver for Real-time Navigation & Guidance

Model:	NovAtel OEM3 Single Frequency Receiver
Type:	SPS (L1 band), 24-channel, C/A code at 1575.42 MHz, S code at 0.5625 MHz, Real-time differential.
Sensitivity:	-132 dBm, 0.5 second update
Accuracy:	Manufacturer's stated accuracy is better than 5 metres real-time

The antenna for the GPS guidance system is mounted on the tail fin of the helicopter.

Airborne Receiver for Flight Path Recovery

Model:	NovAtel OEM4 Dual Frequency Receiver
Type:	Code and carrier tracking of L1 band, 12-channel, dual frequency C/A code at 1575.2 MHz, and L2 P-code 1227 MHz
Sensitivity:	0.5 second update
Accuracy:	Manufacturer's stated accuracy for differential corrected GPS is better than 1 metre

The antenna for the GPS flight path recovery system is mounted on the nose of the EM bird.

Primary Base Station for Post-Survey Differential Correction

Model:	NovAtel Millennium
Type:	Code and carrier tracking of L1-C/A code at 1575.42 MHz and L2-P code at 1227.0 MHz. Dual frequency, 24-channel
Sample rate:	1.0 second update
Accuracy:	Better than 1 metre in differential mode

Secondary GPS Base Station

Model:	Marconi Allstar OEM, CMT-1200 (integrated into the CF1 unit)
Type:	Code and carrier tracking of L1 band, 12-channel, C/A code at 1575.42 MHz
Sensitivity:	-90 dBm, 1.0 second update
Accuracy:	Manufacturer's stated accuracy for differential corrected GPS is 2 metres.

The NovAtel OEM3 is a line of sight, satellite navigation system that utilizes time-coded signals from at least four of forty-eight available satellites. Both Russian GLONASS and American NAVSTAR satellite constellations are used to calculate the position and to provide real time guidance to the helicopter. For flight path processing a NovAtel OEM4 was used as the mobile receiver. A NovAtel Millennium duel frequency system was used as the primary base station receiver. The base station was located at WGS84 latitude 48° 05' 40.93'' N, longitude 105° 34' 23.20'' W and 594.4 metres above the ellipsoid. The mobile and base station raw XYZ data were recorded, thereby permitting post-survey differential corrections for theoretical accuracies of better than 2 metres. A Marconi Allstar GPS unit was used as a secondary (back-up) base station.

Radar Altimeter

Manufacturer:	Honeywell/Sperry
Model:	RT330
Type:	Short pulse modulation, 4.3 GHz
Sensitivity:	0.3 m

The radar altimeter measures the vertical distance between the helicopter and the ground. This information is used in the processing algorithm that determines conductor depth.

Barometric Pressure and Temperature Sensors

Model:	DIGHEM D 1300	
Type:	Motorola MPX4115AP analog pressure sensor AD592AN high-impedance remote temperature sensors	
Sensitivity:	Pressure: Temperature:	150 mV/kPa 100 mV/°C or 10 mV/°C (selectable)
Sample rate:	10 per second	

The D1300 circuit is used in conjunction with one barometric sensor and up to three temperature sensors. Two sensors (baro and temp) are installed in the EM console in the aircraft, to monitor pressure and internal operating temperatures.

Laser Altimeter

Manufacturer:	Optech
Model:	G150
Type:	Fixed pulse repetition rate of 2 kHz
Sensitivity:	±5 cm from 10ºC to 30ºC ±10 cm from -20ºC to +50ºC

The laser altimeter is housed in the EM bird, and measures the distance from the EM bird to ground, except in areas of dense tree cover.

Digital Data Acquisition System

Manufacturer: Fugro Airborne Surveys

Model: HELIDAS

Recorder: San Disk compact flash card (PCMCIA) and IBM Microdrive

The data are stored on flash cards and microdrives and are transfered to the field workstation PC at the survey base for verification, backup and preparation of in-field products.

Flight Path Video Recording System

Recorder: Panasonic AG-720

Fiducial numbers are recorded continuously and are displayed on the margin of each image. This procedure ensures accurate correlation of analog and digital data with respect to visible features on the ground.

4. QUALITY CONTROL AND IN-FIELD PROCESSING

Digital data for each flight were transferred to the field workstation, in order to verify data quality and completeness. A database was created and updated using Geosoft Oasis Montaj and proprietary Fugro Atlas software. This allowed the field personnel to calculate, display and verify the positional and geophysical data.

In-field processing of Fugro survey data consists of differential corrections to the airborne GPS data, verification of EM calibrations, drift correction of the raw airborne EM data, spike rejection and filtering of all geophysical and ancillary data, verification of flight videos, calculation of preliminary resistivity data, diurnal correction, and preliminary leveling of magnetic data.

All data, including base station records, were checked on a daily basis, to ensure compliance with the survey contract specifications. Reflights were required if any of the standard specifications were not met.

5. DATA PROCESSING

Flight Path Recovery

The raw range data from at least four satellites are simultaneously recorded by both the base and mobile GPS units. The geographic positions of both units, relative to the model ellipsoid, are calculated from this information. Differential corrections, which are obtained from the base station, are applied to the mobile unit data to provide a post-flight track of the aircraft, accurate to within 2 m. Speed checks of the flight path are also carried out to determine if there are any spikes or gaps in the data.

The corrected WGS84 latitude/longitude coordinates are transformed to the coordinate system used on the final maps. Images or plots are then created to provide a visual check of the flight path.

Electromagnetic Data/Apparent Resistivity

EM data are processed at the recorded sample rate of 10 samples/second. Spheric rejection median and Hanning filters were applied to reduce noise to acceptable levels.

The apparent resistivity in ohm-m were generated from the in-phase and quadrature EM components for all of the coplanar frequencies, using a pseudo-layer half-space model. The inputs to the resistivity algorithm are the inphase and quadrature amplitudes of the secondary field. The algorithm calculates the apparent resistivity in ohm-m, and the apparent height of the bird above the conductive source. Any difference between the

apparent height and the true height, as measured by the radar altimeter, is called the pseudo-layer and reflects the difference between the real geology and a homogeneous halfspace. This difference is often attributed to the presence of a highly resistive upper layer. Any errors in the altimeter reading, caused by heavy tree cover, are included in the pseudo-layer and do not affect the resistivity calculation. The apparent depth estimates, however, will reflect the altimeter errors. Apparent resistivity calculated in this manner may behave quite differently from those calculated using other models.

In areas of high magnetic permeability or dielectric permittivity, the calculated resistivities will be erroneously high. Various algorithms and inversion techniques can be used to partially correct for this effect.

The preliminary apparent resistivity maps and images were carefully inspected to identify any lines or line segments that might require base level adjustments. Subtle changes between in-flight calibrations of the system can result in line-to-line differences that are more recognizable in resistive (low signal amplitude) areas. Manual leveling was carried out to eliminate or minimize resistivity differences that can be attributed, in part, to changes in operating temperatures. These leveling adjustments were usually very subtle, and do not result in the degradation of discrete anomalies.

Apparent resistivity grids, which display the conductive properties of the survey areas, were produced from the 400 Hz, 1800 Hz, 8200 Hz, 40,000 Hz and 140,000 Hz coplanar data, and for the 3300 Hz coaxial data. The calculated resistivities for all six frequencies are included in the XYZ and grid archives. Values are in ohm-metres on all final products.

Total Magnetic Field

The aeromagnetic data were inspected in grid and profile format. Spikes were removed manually with the aid of a fourth difference calculation. A Geometrics G822 cesium vapour magnetometer was operated at the survey base to record diurnal variations of the earth's magnetic field. The clock of the base station was synchronized with that of the airborne system to permit subsequent removal of diurnal drift. The data were inspected for spikes and filtered. The filtered diurnal data were subtracted from the total field magnetic data. Grids of the diurnally corrected aeromagnetic data were created and contoured. A lag correction was applied to the magnetic data. Manual adjustments were applied to any lines that required leveling, as indicated by shadowed images of both the total field magnetic data and the calculated vertical gradient data. A microleveling algorithm was used to make any remaining subtle leveling adjustments.

Contour, Colour and Shadow Map Displays

The geophysical data are interpolated onto a regular grid using a modified Akima spline technique. The resulting grid is suitable for image processing and generation of contour maps. The grid cell size was 20% of the line interval; 40 metres for the 200 metre spaced portion of the survey area, 20 metres for the 100 metre spaced detail area.

Colour maps are produced by interpolating the grid down to the pixel size. The parameter is then incremented with respect to specific amplitude ranges to provide colour "contour" maps.

Monochromatic shadow maps or images can be generated by employing an artificial sun to cast shadows on a surface defined by the geophysical grid. There are many variations in the shadowing technique. These techniques can be applied to total field or enhanced magnetic data, magnetic derivatives, resistivity, etc. The shadowing technique is also used as a quality control method to detect subtle changes between lines.

Resistivity-depth Sections (optional)

The apparent resistivities for all frequencies can be displayed simultaneously as coloured resistivity-depth sections. Usually, only the coplanar data are displayed as the close frequency separation between the coplanar and adjacent coaxial data tends to distort the section. The sections can be plotted using the topographic elevation profile as the surface. The digital terrain values, in metres a.m.s.l., can be calculated from the GPS Z-value or barometric altimeter, minus the aircraft radar altimeter.

Resistivity-depth sections can be generated in three formats:

(1) Sengpiel resistivity sections, where the apparent resistivity for each frequency is plotted at the depth of the centroid of the in-phase current flow[1]; and,

(2) Differential resistivity sections, where the differential resistivity is plotted at the differential depth[2].

---

[1] Sengpiel, K.P., 1988, Approximate Inversion of Airborne EM Data from Multilayered Ground: Geophysical Prospecting 36, 446-459.

(3) Occam[3] or Multi-layer[4] inversion.

Both the Sengpiel and differential methods are derived from the pseudo-layer half-space model. Both yield a coloured resistivity-depth section that attempts to portray a smoothed approximation of the true resistivity distribution with depth. Resistivity-depth sections are most useful in conductive layered situations, but may be unreliable in areas of moderate to high resistivity where signal amplitudes are weak. In areas where in-phase responses have been suppressed by the effects of magnetite, or adversely affected by cultural features, the computed resistivities shown on the sections may be unreliable.

Both the Occam and multi-layer inversions compute the layered earth resistivity model that would best match the measured EM data. The Occam inversion uses a series of thin, fixed layers (usually 20 x 5m and 10 x 10m layers) and computes resistivities to fit the EM data. The multi-layer inversion computes the resistivity and thickness for each of a defined number of layers (typically 3-5 layers) to best fit the data.

---

[2] Huang, H. and Fraser, D.C., 1993, Differential Resistivity Method for Multi-frequency Airborne EM Sounding: presented at Intern. Airb. EM Workshop, Tucson, Ariz.

[3] Constable et al, 1987, Occam's inversion: a practical algorithm for generating smooth models from electromagnetic sounding data: Geophysics, 52, 289-300.

[4] Huang H., and Palacky, G.J., 1991, Damped least-squares inversion of time domain airborne EM data based on singular value decomposition: Geophysical Prospecting, 39, 827-844.

6. PRODUCTS

This section lists the final maps and products that have been provided under the terms of the survey agreement. Other products can be prepared from the existing dataset, if requested. These include magnetic enhancements or derivatives, percent magnetite, resistivities corrected for magnetic permeability and/or dielectric permittivity, digital terrain, resistivity-depth sections, inversions, and overburden thickness.

Base Maps

Base maps of the survey area were produced by scanning published topographic maps to a BMP format. This process provides a relatively accurate, distortion free base that facilitates correlation of the navigation data to the map coordinate system. The topographic files were combined with geophysical data for plotting the final maps. All maps were created using the following parameters:

Projection Description:

Datum:	NAD 27
Ellipsoid:	Clarke 1866
DX,DY,ZY shift	8 -159 -175
Projection:	UTM Zone 13N
Central Meridian:	105° West
False Northing:	0
False Easting:	500000
Scale Factor:	0.9996

The following parameters are presented on 1 map sheet at a scale of 1:24,000. Preliminary products are not listed.

Final Products

Colour Maps (2 copies) at 1:24000

Apparent Resistivity 400 Hz
Apparent Resistivity 1800 Hz
Apparent Resistivity 3300 Hz
Apparent Resistivity 8200 Hz
Apparent Resistivity 40,000 Hz
Apparent Resistivity 140,000 Hz
Total Magnetic Field

Additional Products

Digital Archive on CD-ROM	3 copies
Survey Report	3 copies
Flight Path Video (VHS and DVD)	All flights

7. CONCLUSIONS AND RECOMMENDATIONS

This report provides a description of the equipment, data processing procedures and logistics of the survey.

The various maps included with this report display the magnetic and conductive properties of the survey area. It is recommended that a complete assessment and detailed evaluation of the survey results be carried out, in conjunction with all available geophysical, geological and geochemical information.

It is also recommended that image processing of existing geophysical data be considered, in order to extract the maximum amount of information from the survey results. Current software and imaging techniques often provide valuable information on structure and lithology, which may not be clearly evident on the contour and colour maps. These techniques can yield images that define subtle, but significant, structural details.

Respectfully submitted,

FUGRO AIRBORNE SURVEYS CORP.

Michael Cain, P. Eng.
Geophysicist

APPENDIX A
LIST OF PERSONNEL

The following personnel were involved in the acquisition, processing, interpretation and presentation of data, relating to a RESOLVE airborne geophysical survey carried out for the U. S. Geological Survey, over the East Poplar Oil Fields, Montana.

David Miles	Manager, Helicopter Operations
Emily Farquhar	Manager, Data Processing and Interpretation
Bill Brown	Sales and Marketing
Michael Cain	Project Geophysicist
Igor Sram	Field Geophysicist
Darcy Blouin	Geophysical Operator
Bill Hofestede	Pilot (Questral Helicopters Ltd.)
Lyn Vanderstarren	Drafting Supervisor
Albina Tonello	Secretary/Expeditor

The survey consisted of 1645 km of coverage, flown from August 12th to 14th, 2004.

All personnel are employees of Fugro Airborne Surveys, except for the pilot who is an employee of Questral Helicopters Ltd.

APPENDIX B
ARCHIVE DESCRIPTION

This CD-ROM contains final data archives of an airborne survey conducted by Fugro Airborne Surveys on behalf of the U. S. Geological Survey.

CD Archive number: CCD02231

Fugro Airborne Surveys Job #04034

The archives contain three directories.

1. Line Data: Geosoft GDB database with archive description.

2. Grids: Grids in Geosoft GRD format for the following parameters:
    1. Magnetic total field
    2. Digital terrain model
    3. 6 resistivities

3. Report: A digital copy of the operations report in Word and PDF format

Projection Description:

Datum:	NAD27
Ellipsoid:	Clarke 1866
Projection:	UTM Zone 13N
Central Meridian:	105º West
False Northing:	0
False Easting:	500000
Scale Factor:	0.9996
WGS84 to Local Conversion:	Molodensky
X,Y,Z Datum Shifts:	8 -159 -175

- Appendix B.2 -

EM PARAMETERS

orientation	FREQUENCY nominal	actual	COIL SPACING
coplanar	400 Hz	391 Hz	7.9 m
coplanar	1 800 Hz	1 801 Hz	7.9 m
coaxial	3 300 Hz	3 326 Hz	9.0 m
coplanar	8 200 Hz	8 162 Hz	7.9 m
coplanar	40 000 Hz	39 130 Hz	7.9 m
coplanar	140 000 Hz	132 640 Hz	7.9 m

DATABASE : 03069_BEXAR.GDB

NUMBER OF DATABASE CHANNELS : 95

1	ALTBIRDM	BIRD RADAR ALTIMETER (METRES)
2	ALTBIRDR	BIRD RADAR ALTIMETER RAW (METRES)
3	ALTLASM	BIRD LASER ALTIMETER PROCESSED (METRES)
4	ALTLASR	BIRD LASER ALTIMETER RAW (METRES)
5	BALT	BAROMETRIC ALTIMETER RAW (METRES)
6	CEN140k	CENTROID DEPTH 140K Hz
7	CEN1800	CENTROID DEPTH 1800 Hz
8	CEN40k	CENTROID DEPTH 40K Hz
9	CEN400	CENTROID DEPTH 400 Hz
10	CEN8200	CENTROID DEPTH 8200 Hz
11	CPI140K	COPLANAR INPHASE FULLY PROCESSED 140K Hz
12	CPI1800	COPLANAR INPHASE FULLY PROCESSED 1800 Hz
13	CPI40K	COPLANAR INPHASE FULLY PROCESSED 40K Hz
14	CPI400	COPLANAR INPHASE FULLY PROCESSED 400 Hz
15	CPI8200	COPLANAR INPHASE FULLY PROCESSED 8200 Hz
16	CPQ140K	COPLANAR QUADRATURE FULLY PROCESSED 140K Hz
17	CPQ1800	COPLANAR QUADRATURE FULLY PROCESSED 1800 Hz
18	CPQ40K	COPLANAR QUADRATURE FULLY PROCESSED 40K Hz
19	CPQ400	COPLANAR QUADRATURE FULLY PROCESSED 400 Hz
20	CPQ8200	COPLANAR QUADRATURE FULLY PROCESSED 8200 Hz
21	CXI3300	COAXIAL INPHASE FULLY PROCESSED 3300 Hz
22	CXQ3300	COAXIAL QUADRATURE FULLY PROCESSED 3300 Hz
23	CPPL1	COPLANAR POWERLINE MONITOR
24	CPPL2	COPLANAR POWERLINE MONITOR
25	DATE	FLIGHT DATE
26	DDEP140K	DIFFERENTIAL DEPTH 140K Hz FILTERED
27	DDEP1800	DIFFERENTIAL DEPTH 1800Hz FILTERED
28	DDEP40K	DIFFERENTIAL DEPTH 40K Hz FILTERED
29	DDEP400	DIFFERENTIAL DEPTH 400 Hz FILTERED
30	DDEP8200	DIFFERENTIAL DEPTH 8200 Hz FILTERED
31	DEP140K	APPARENT DEPTH 140K Hz FILTERED
32	DEP1800	APPARENT DEPTH 1800Hz FILTERED
33	DEP40K	APPARENT DEPTH 40K Hz FILTERED
34	DEP3300	APPARENT DEPTH 3300 Hz FILTERED
35	DEP400	APPARENT DEPTH 400 Hz FILTERED
36	DEP8200	APPARENT DEPTH 8200 Hz FILTERED
37	DIURNAL	DIURNAL CORRECTION
38	DRES140K	DIFFERENTIAL RESISTIVITY 140K Hz FILTERED
39	DRES1800	DIFFERENTIAL RESISTIVITY 1800 Hz FILTERED
40	DRES40K	DIFFERENTIAL RESISTIVITY 40K Hz FILTERED
41	DRES400	DIFFERENTIAL RESISTIVITY 400 Hz FILTERED
42	DRES8200	DIFFERENTIAL RESISTIVITY 8200 Hz FILTERED
43	DTM	DIGITAL TERRAIN MODEL
44	FID	FIDUCIAL COUNTER
45	Flight	FLIGHT NUMBER
46	GPSZ	RAW GPS ELEVATION
47	L140I	BASE LEVELED INPHASE 140K Hz
48	L140Q	BASE LEVELED QUADRATURE 140K Hz

```
   49 - L1K8I            BASE LEVELED INPHASE 1800 Hz
   50 - L1K8Q            BASE LEVELED QUADRATURE 1800 Hz
   51 - L3X3I            BASE LEVELED INPHASE 3300 Hz
   52 - L3X3Q            BASE LEVELED QUADRATURE 3300 Hz
   53 - L40KI            BASE LEVELED INPHASE 400 Hz
   54 - L40KQ            BASE LEVELED QUADRATURE 40K Hz
   55 - L400I            BASE LEVELED INPHASE 400 Hz
   56 - L400Q            BASE LEVELED QUADRATURE 400 Hz
   57 - L8K2I            BASE LEVELED INPHASE 8200 Hz
   58 - L8K2Q            BASE LEVELED QUADRATURE 8200 Hz
   59 - LAT              WGS84 LATITUDE
   60 - LON              WGS84 LONGITUDE
   61 - LINE             LINE NUMBER
   62 - MAGD             DIURNAL CORRECTED MAG
   63 - MAGRAW           RAW MAG
   64 - MAG_IGRF         MAG IGRF REMOVED USING Z ALTITUDE
   65 - MAG              FINAL MAG
   66 - RES140K          RESISTIVITY 140K Hz
   67 - RES1800          RESISTIVITY 1800 Hz
   68 - RES40K           RESISTIVITY 40K Hz
   69 - RES3300          RESISTIVITY 3300 Hz
   70 - RES400           RESISTIVITY 400 Hz
   71 - RES8200          RESISTIVITY 8200 Hz
   72 - UTC              UTC TIME
   73 - X                FINAL BIRD UTM X CLARK 1866 (NAD27)
   74 - X1               FINAL BIRD UTM X CLARK 1866 (NAD27) (NO DETAIL)
   75 - X2               FINAL BIRD UTM X CLARK 1866 (NAD27) (NORTH DETAIL)
   76 - X3               FINAL BIRD UTM X CLARK 1866 (NAD27) (SOUTH DETAIL)
   77 - Y                FINAL BIRD UTM Y CLARK 1866 (NAD27)
   78 - Y1               FINAL BIRD UTM Y CLARK 1866 (NAD27) (NO DETAIL)
   79 - Y2               FINAL BIRD UTM Y CLARK 1866 (NAD27) (NORTH DETAIL)
   80 - Y3               FINAL BIRD UTM Y CLARK 1866 (NAD27) (SOUTH DETAIL)
   81 - X_HELI           UTM X FROM HELI GPS CLARK 1866 (NAD27)
   82 - Y_HELI           UTM X FROM HELI GPS CLARK 1866 (NAD27)
   83 - Z                FINAL GPS ELEVATION
   84 - _140I            RAW INPHASE 140K Hz
   85 - _140Q            RAW QUADRATURE 140K Hz
   86 - _1K8I            RAW INPHASE 1800 Hz
   87 - _1K8Q            RAW QUADRATURE 1800 Hz
   88 - _3X3I            RAW INPHASE 3300 Hz
   89 - _3X3Q            RAW QUADRATURE 3300 Hz
   90 - _40KI            RAW INPHASE 40K Hz
   91 - _40KQ            RAW QUADRATURE 40K Hz
   92 - _400I            RAW INPHASE 400 Hz
   93 - _400Q            RAW QUADRATURE 400 Hz
   94 - _8K2I            RAW INPHASE 8200 Hz
   95 - _8K2Q            RAW QUADRATURE 8200 Hz
==================================================
```

APPENDIX C
BACKGROUND INFORMATION

Electromagnetics

Fugro electromagnetic responses fall into two general classes, discrete and broad. The discrete class consists of sharp, well-defined anomalies from discrete conductors such as sulphide lenses and steeply dipping sheets of graphite and sulphides. The broad class consists of wide anomalies from conductors having a large horizontal surface such as flatly dipping graphite or sulphide sheets, saline water-saturated sedimentary formations, conductive overburden and rock, kimberlite pipes and geothermal zones. A vertical conductive slab with a width of 200 m would straddle these two classes.

The vertical sheet (half plane) is the most common model used for the analysis of discrete conductors. All anomalies plotted on the geophysical maps are analyzed according to this model. The following section entitled **Discrete Conductor Analysis** describes this model in detail, including the effect of using it on anomalies caused by broad conductors such as conductive overburden.

The conductive earth (half-space) model is suitable for broad conductors. Resistivity contour maps result from the use of this model. A later section entitled **Resistivity Mapping** describes the method further, including the effect of using it on anomalies caused by discrete conductors such as sulphide bodies.

Geometric Interpretation

The geophysical interpreter attempts to determine the geometric shape and dip of the conductor. Figure C-1 shows typical HEM anomaly shapes which are used to guide the geometric interpretation.

Discrete Conductor Analysis

The EM anomalies appearing on the electromagnetic map are analyzed by computer to give the conductance (i.e., conductivity-thickness product) in siemens (mhos) of a vertical sheet model. This is done regardless of the interpreted geometric shape of the conductor. This is not an unreasonable procedure, because the computed conductance increases as the electrical quality of the conductor increases, regardless of its true shape. DIGHEM anomalies are divided into seven grades of conductance, as shown in Table C-1. The conductance in siemens (mhos) is the reciprocal of resistance in ohms.

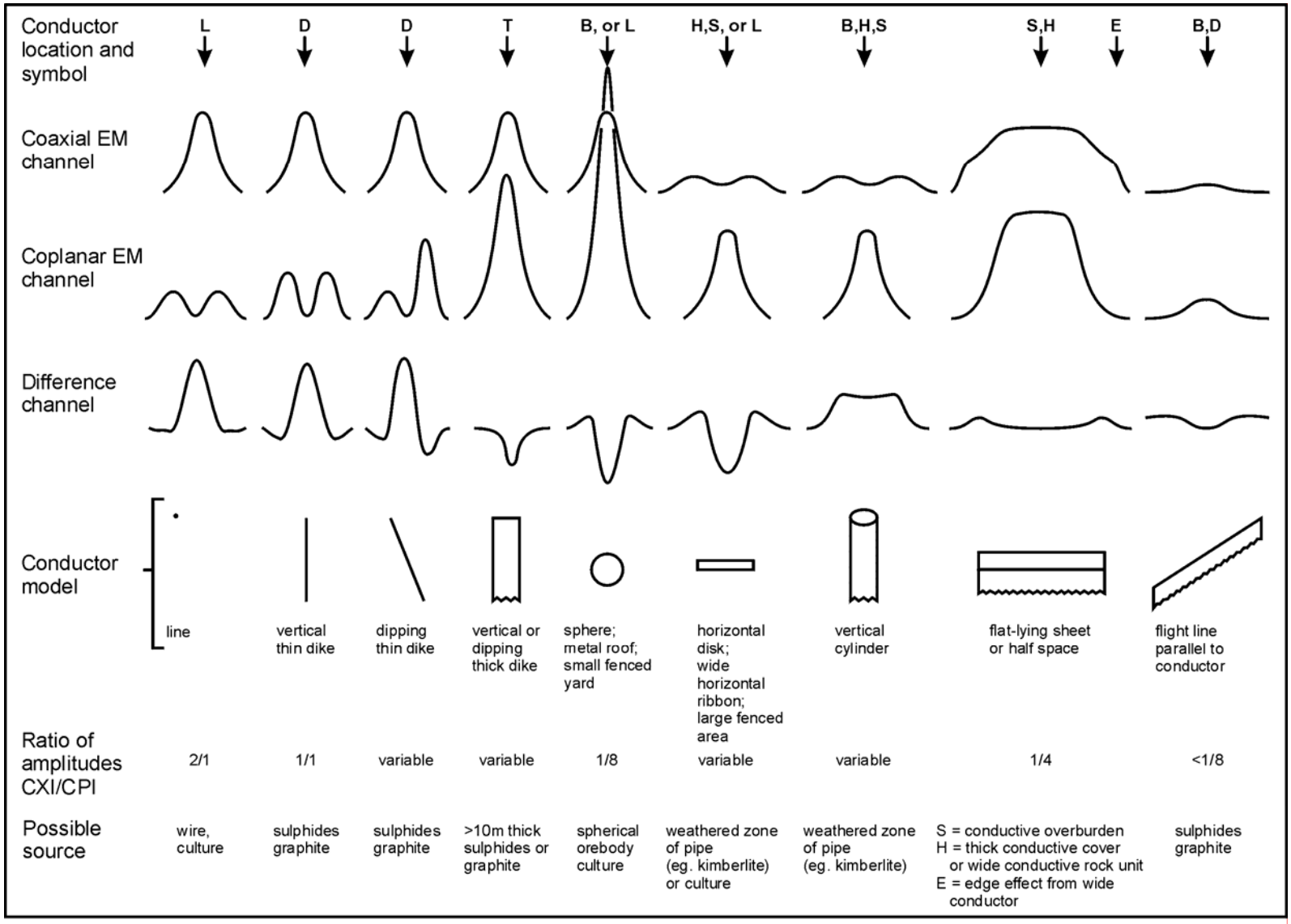

Typical DIGHEM anomaly shapes

Figure C-1

The conductance value is a geological parameter because it is a characteristic of the conductor alone. It generally is independent of frequency, flying height or depth of burial, apart from the averaging over a greater portion of the conductor as height increases. Small anomalies from deeply buried strong conductors are not confused with small anomalies from shallow weak conductors because the former will have larger conductance values.

Table C-1. EM Anomaly Grades

Anomaly Grade	Siemens
7	> 100
6	50 - 100
5	20 - 50
4	10 - 20
3	5 - 10
2	1 - 5
1	< 1

Conductive overburden generally produces broad EM responses which may not be shown as anomalies on the geophysical maps. However, patchy conductive overburden in otherwise resistive areas can yield discrete anomalies with a conductance grade (cf. Table C-1) of 1, 2 or even 3 for conducting clays which have resistivities as low as 50 ohm-m. In areas where ground resistivities are below 10 ohm-m, anomalies caused by weathering variations and similar causes can have any conductance grade. The anomaly shapes from the multiple coils often allow such conductors to be recognized, and these are indicated by the letters S, H, and sometimes E on the geophysical maps (see EM legend on maps).

For bedrock conductors, the higher anomaly grades indicate increasingly higher conductances. Examples: the New Insco copper discovery (Noranda, Canada) yielded a grade 5 anomaly, as did the neighbouring copper-zinc Magusi River ore body; Mattabi (copper-zinc, Sturgeon Lake, Canada) and Whistle (nickel, Sudbury, Canada) gave grade 6; and the Montcalm nickel-copper discovery (Timmins, Canada) yielded a grade 7 anomaly. Graphite and sulphides can span all grades but, in any particular survey area, field work may show that the different grades indicate different types of conductors.

Strong conductors (i.e., grades 6 and 7) are characteristic of massive sulphides or graphite. Moderate conductors (grades 4 and 5) typically reflect graphite or sulphides of a less massive character, while weak bedrock conductors (grades 1 to 3) can signify poorly connected graphite or heavily disseminated sulphides. Grades 1 and 2 conductors may not respond to ground EM equipment using frequencies less than 2000 Hz.

The presence of sphalerite or gangue can result in ore deposits having weak to moderate conductances. As an example, the three million ton lead-zinc deposit of Restigouche Mining Corporation near Bathurst, Canada, yielded a well-defined grade 2 conductor. The 10 percent by volume of sphalerite occurs as a coating around the fine grained massive pyrite, thereby inhibiting electrical conduction. Faults, fractures and shear zones may produce anomalies that typically have low conductances (e.g., grades 1 to 3). Conductive rock formations can yield anomalies of any conductance grade. The conductive materials in such rock formations can be salt water, weathered products such as clays, original depositional clays, and carbonaceous material.

- Appendix C.4 -

For each interpreted electromagnetic anomaly on the geophysical maps, a letter identifier and an interpretive symbol are plotted beside the EM grade symbol. The horizontal rows of dots, under the interpretive symbol, indicate the anomaly amplitude on the flight record. The vertical column of dots, under the anomaly letter, gives the estimated depth. In areas where anomalies are crowded, the letter identifiers, interpretive symbols and dots may be obliterated. The EM grade symbols, however, will always be discernible, and the obliterated information can be obtained from the anomaly listing appended to this report.

The purpose of indicating the anomaly amplitude by dots is to provide an estimate of the reliability of the conductance calculation. Thus, a conductance value obtained from a large ppm anomaly (3 or 4 dots) will tend to be accurate whereas one obtained from a small ppm anomaly (no dots) could be quite inaccurate. The absence of amplitude dots indicates that the anomaly from the coaxial coil-pair is 5 ppm or less on both the in-phase and quadrature channels. Such small anomalies could reflect a weak conductor at the surface or a stronger conductor at depth. The conductance grade and depth estimate illustrates which of these possibilities fits the recorded data best.

The conductance measurement is considered more reliable than the depth estimate. There are a number of factors that can produce an error in the depth estimate, including the averaging of topographic variations by the altimeter, overlying conductive overburden, and the location and attitude of the conductor relative to the flight line. Conductor location and attitude can provide an erroneous depth estimate because the stronger part of the conductor may be deeper or to one side of the flight line, or because it has a shallow dip. A heavy tree cover can also produce errors in depth estimates. This is because the depth estimate is computed as the distance of bird from conductor, minus the altimeter reading. The altimeter can lock onto the top of a dense forest canopy. This situation yields an erroneously large depth estimate but does not affect the conductance estimate.

Dip symbols are used to indicate the direction of dip of conductors. These symbols are used only when the anomaly shapes are unambiguous, which usually requires a fairly resistive environment.

A further interpretation is presented on the EM map by means of the line-to-line correlation of bedrock anomalies, which is based on a comparison of anomaly shapes on adjacent lines. This provides conductor axes that may define the geological structure over portions of the survey area. The absence of conductor axes in an area implies that anomalies could not be correlated from line to line with reasonable confidence.

The electromagnetic anomalies are designed to provide a correct impression of conductor quality by means of the conductance grade symbols. The symbols can stand alone with geology when planning a follow-up program. The actual conductance values are printed in the attached anomaly list for those who wish quantitative data. The anomaly ppm and depth are indicated by inconspicuous dots which should not distract from the conductor patterns, while being helpful to those who wish this information. The map provides an interpretation of conductors in terms of length, strike and dip, geometric shape,

conductance, depth, and thickness. The accuracy is comparable to an interpretation from a high quality ground EM survey having the same line spacing.

The appended EM anomaly list provides a tabulation of anomalies in ppm, conductance, and depth for the vertical sheet model. No conductance or depth estimates are shown for weak anomalous responses that are not of sufficient amplitude to yield reliable calculations.

Since discrete bodies normally are the targets of EM surveys, local base (or zero) levels are used to compute local anomaly amplitudes. This contrasts with the use of true zero levels which are used to compute true EM amplitudes. Local anomaly amplitudes are shown in the EM anomaly list and these are used to compute the vertical sheet parameters of conductance and depth.

Questionable Anomalies

The EM maps may contain anomalous responses that are displayed as asterisks (*). These responses denote weak anomalies of indeterminate conductance, which may reflect one of the following: a weak conductor near the surface, a strong conductor at depth (e.g., 100 to 120 m below surface) or to one side of the flight line, or aerodynamic noise. Those responses that have the appearance of valid bedrock anomalies on the flight profiles are indicated by appropriate interpretive symbols (see EM legend on maps). The others probably do not warrant further investigation unless their locations are of considerable geological interest.

The Thickness Parameter

A comparison of coaxial and coplanar shapes can provide an indication of the thickness of a steeply dipping conductor. The amplitude of the coplanar anomaly (e.g., CPI channel) increases relative to the coaxial anomaly (e.g., CXI) as the apparent thickness increases, i.e., the thickness in the horizontal plane. (The thickness is equal to the conductor width if the conductor dips at 90 degrees and strikes at right angles to the flight line.) This report refers to a conductor as thin when the thickness is likely to be less than 3 m, and thick when in excess of 10 m. Thick conductors are indicated on the EM map by parentheses "( )". For base metal exploration in steeply dipping geology, thick conductors can be high priority targets because many massive sulphide ore bodies are thick. The system cannot sense the thickness when the strike of the conductor is subparallel to the flight line, when the conductor has a shallow dip, when the anomaly amplitudes are small, or when the resistivity of the environment is below 100 ohm-m.

Resistivity Mapping

Resistivity mapping is useful in areas where broad or flat lying conductive units are of interest. One example of this is the clay alteration which is associated with Carlin-type deposits in the south west United States. The resistivity parameter was able to identify the

clay alteration zone over the Cove deposit. The alteration zone appeared as a strong resistivity low on the 900 Hz resistivity parameter. The 7,200 Hz and 56,000 Hz resistivities showed more detail in the covering sediments, and delineated a range front fault. This is typical in many areas of the south west United States, where conductive near surface sediments, which may sometimes be alkalic, attenuate the higher frequencies.

Resistivity mapping has proven successful for locating diatremes in diamond exploration. Weathering products from relatively soft kimberlite pipes produce a resistivity contrast with the unaltered host rock. In many cases weathered kimberlite pipes were associated with thick conductive layers that contrasted with overlying or adjacent relatively thin layers of lake bottom sediments or overburden.

Areas of widespread conductivity are commonly encountered during surveys. These conductive zones may reflect alteration zones, shallow-dipping sulphide or graphite-rich units, saline ground water, or conductive overburden. In such areas, EM amplitude changes can be generated by decreases of only 5 m in survey altitude, as well as by increases in conductivity. The typical flight record in conductive areas is characterized by in-phase and quadrature channels that are continuously active. Local EM peaks reflect either increases in conductivity of the earth or decreases in survey altitude. For such conductive areas, apparent resistivity profiles and contour maps are necessary for the correct interpretation of the airborne data. The advantage of the resistivity parameter is that anomalies caused by altitude changes are virtually eliminated, so the resistivity data reflect only those anomalies caused by conductivity changes. The resistivity analysis also helps the interpreter to differentiate between conductive bedrock and conductive overburden. For example, discrete conductors will generally appear as narrow lows on the contour map and broad conductors (e.g., overburden) will appear as wide lows.

The apparent resistivity is calculated using the pseudo-layer (or buried) half-space model defined by Fraser (1978)[5]. This model consists of a resistive layer overlying a conductive half-space. The depth channels give the apparent depth below surface of the conductive material. The apparent depth is simply the apparent thickness of the overlying resistive layer. The apparent depth (or thickness) parameter will be positive when the upper layer is more resistive than the underlying material, in which case the apparent depth may be quite close to the true depth.

The apparent depth will be negative when the upper layer is more conductive than the underlying material, and will be zero when a homogeneous half-space exists. The apparent depth parameter must be interpreted cautiously because it will contain any errors that might exist in the measured altitude of the EM bird (e.g., as caused by a dense tree cover). The inputs to the resistivity algorithm are the in-phase and quadrature components of the coplanar coil-pair. The outputs are the apparent resistivity of the conductive half-space (the source) and the sensor-source distance. The flying height is not an input variable, and the

[5] Resistivity mapping with an airborne multicoil electromagnetic system: Geophysics, v. 43, p.144-172

output resistivity and sensor-source distance are independent of the flying height when the conductivity of the measured material is sufficient to yield significant in-phase as well as quadrature responses. The apparent depth, discussed above, is simply the sensor-source distance minus the measured altitude or flying height. Consequently, errors in the measured altitude will affect the apparent depth parameter but not the apparent resistivity parameter.

The apparent depth parameter is a useful indicator of simple layering in areas lacking a heavy tree cover. Depth information has been used for permafrost mapping, where positive apparent depths were used as a measure of permafrost thickness. However, little quantitative use has been made of negative apparent depths because the absolute value of the negative depth is not a measure of the thickness of the conductive upper layer and, therefore, is not meaningful physically. Qualitatively, a negative apparent depth estimate usually shows that the EM anomaly is caused by conductive overburden. Consequently, the apparent depth channel can be of significant help in distinguishing between overburden and bedrock conductors.

Interpretation in Conductive Environments

Environments having low background resistivities (e.g., below 30 ohm-m for a 900 Hz system) yield very large responses from the conductive ground. This usually prohibits the recognition of discrete bedrock conductors. However, Fugro data processing techniques produce three parameters that contribute significantly to the recognition of bedrock conductors in conductive environments. These are the in-phase and quadrature difference channels (DIFI and DIFQ, which are available only on systems with “common” frequencies on orthogonal coil pairs), and the resistivity and depth channels (RES and DEP) for each coplanar frequency.

The EM difference channels (DIFI and DIFQ) eliminate most of the responses from conductive ground, leaving responses from bedrock conductors, cultural features (e.g., telephone lines, fences, etc.) and edge effects. Edge effects often occur near the perimeter of broad conductive zones. This can be a source of geologic noise. While edge effects yield anomalies on the EM difference channels, they do not produce resistivity anomalies. Consequently, the resistivity channel aids in eliminating anomalies due to edge effects. On the other hand, resistivity anomalies will coincide with the most highly conductive sections of conductive ground, and this is another source of geologic noise. The recognition of a bedrock conductor in a conductive environment therefore is based on the anomalous responses of the two difference channels (DIFI and DIFQ) and the resistivity channels (RES). The most favourable situation is where anomalies coincide on all channels.

The DEP channels, which give the apparent depth to the conductive material, also help to determine whether a conductive response arises from surficial material or from a conductive zone in the bedrock. When these channels ride above the zero level on the depth profiles (i.e., depth is negative), it implies that the EM and resistivity profiles are responding primarily to a conductive upper layer, i.e., conductive overburden. If the DEP channels are below the zero level, it indicates that a resistive upper layer exists, and this usually implies the existence of a bedrock conductor. If the low frequency DEP channel is below the zero level

and the high frequency DEP is above, this suggests that a bedrock conductor occurs beneath conductive cover.

Reduction of Geologic Noise

Geologic noise refers to unwanted geophysical responses. For purposes of airborne EM surveying, geologic noise refers to EM responses caused by conductive overburden and magnetic permeability. It was mentioned previously that the EM difference channels (i.e., channel DIFI for in-phase and DIFQ for quadrature) tend to eliminate the response of conductive overburden.

Magnetite produces a form of geological noise on the in-phase channels. Rocks containing less than 1% magnetite can yield negative in-phase anomalies caused by magnetic permeability. When magnetite is widely distributed throughout a survey area, the in-phase EM channels may continuously rise and fall, reflecting variations in the magnetite percentage, flying height, and overburden thickness. This can lead to difficulties in recognizing deeply buried bedrock conductors, particularly if conductive overburden also exists. However, the response of broadly distributed magnetite generally vanishes on the in-phase difference channel DIFI. This feature can be a significant aid in the recognition of conductors that occur in rocks containing accessory magnetite.

EM Magnetite Mapping

The information content of HEM data consists of a combination of conductive eddy current responses and magnetic permeability responses. The secondary field resulting from conductive eddy current flow is frequency-dependent and consists of both in-phase and quadrature components, which are positive in sign. On the other hand, the secondary field resulting from magnetic permeability is independent of frequency and consists of only an in-phase component that is negative in sign. When magnetic permeability manifests itself by decreasing the measured amount of positive in-phase, its presence may be difficult to recognize. However, when it manifests itself by yielding a negative in-phase anomaly (e.g., in the absence of eddy current flow), its presence is assured. In this latter case, the negative component can be used to estimate the percent magnetite content.

A magnetite mapping technique, based on the low frequency coplanar data, can be complementary to magnetometer mapping in certain cases. Compared to magnetometry, it is far less sensitive but is more able to resolve closely spaced magnetite zones, as well as providing an estimate of the amount of magnetite in the rock. The method is sensitive to 1/4% magnetite by weight when the EM sensor is at a height of 30 m above a magnetitic half-space. It can individually resolve steep dipping narrow magnetite-rich bands which are separated by 60 m. Unlike magnetometry, the EM magnetite method is unaffected by remanent magnetism or magnetic latitude.

The EM magnetite mapping technique provides estimates of magnetite content which are usually correct within a factor of 2 when the magnetite is fairly uniformly distributed. EM

magnetite maps can be generated when magnetic permeability is evident as negative in-phase responses on the data profiles.

Like magnetometry, the EM magnetite method maps only bedrock features, provided that the overburden is characterized by a general lack of magnetite. This contrasts with resistivity mapping which portrays the combined effect of bedrock and overburden.

The Susceptibility Effect

When the host rock is conductive, the positive conductivity response will usually dominate the secondary field, and the susceptibility effect[6] will appear as a reduction in the in-phase, rather than as a negative value. The in-phase response will be lower than would be predicted by a model using zero susceptibility. At higher frequencies the in-phase conductivity response also gets larger, so a negative magnetite effect observed on the low frequency might not be observable on the higher frequencies, over the same body. The susceptibility effect is most obvious over discrete magnetite-rich zones, but also occurs over uniform geology such as a homogeneous half-space.

High magnetic susceptibility will affect the calculated apparent resistivity, if only conductivity is considered. Standard apparent resistivity algorithms use a homogeneous half-space model, with zero susceptibility. For these algorithms, the reduced in-phase response will, in most cases, make the apparent resistivity higher than it should be. It is important to note that there is nothing wrong with the data, nor is there anything wrong with the processing algorithms. The apparent difference results from the fact that the simple geological model used in processing does not match the complex geology.

Measuring and Correcting the Magnetite Effect

Theoretically, it is possible to calculate (forward model) the combined effect of electrical conductivity and magnetic susceptibility on an EM response in all environments. The difficulty lies, however, in separating out the susceptibility effect from other geological effects when deriving resistivity and susceptibility from EM data.

Over a homogeneous half-space, there is a precise relationship between in-phase, quadrature, and altitude. These are often resolved as phase angle, amplitude, and altitude. Within a reasonable range, any two of these three parameters can be used to calculate the half space resistivity. If the rock has a positive magnetic susceptibility, the in-phase component will be reduced and this departure can be recognized by comparison to the other parameters.

---

[6] Magnetic susceptibility and permeability are two measures of the same physical property. Permeability is generally given as relative permeability, μ_r, which is the permeability of the substance divided by the permeability of free space ($4 \pi \times 10^{-7}$). Magnetic susceptibility k is related to permeability by $k=\mu^r-1$. Susceptibility is a unitless measurement, and is usually reported in units of 10^{-6}. The typical range of susceptibilities is –1 for quartz, 130 for pyrite, and up to 5×10^5 for magnetite, in 10^{-6} units (Telford et al, 1986).

The algorithm used to calculate apparent susceptibility and apparent resistivity from HEM data, uses a homogeneous half-space geological model. Non half-space geology, such as horizontal layers or dipping sources, can also distort the perfect half-space relationship of the three data parameters. While it may be possible to use more complex models to calculate both rock parameters, this procedure becomes very complex and time-consuming. For basic HEM data processing, it is most practical to stick to the simplest geological model.

Magnetite reversals (reversed in-phase anomalies) have been used for many years to calculate an “FeO” or magnetite response from HEM data (Fraser, 1981). However, this technique could only be applied to data where the in-phase was observed to be negative, which happens when susceptibility is high and conductivity is low.

Applying Susceptibility Corrections

Resistivity calculations done with susceptibility correction may change the apparent resistivity. High-susceptibility conductors, that were previously masked by the susceptibility effect in standard resistivity algorithms, may become evident. In this case the susceptibility corrected apparent resistivity is a better measure of the actual resistivity of the earth. However, other geological variations, such as a deep resistive layer, can also reduce the in-phase by the same amount. In this case, susceptibility correction would not be the best method. Different geological models can apply in different areas of the same data set. The effects of susceptibility, and other effects that can create a similar response, must be considered when selecting the resistivity algorithm.

Susceptibility from EM vs Magnetic Field Data

The response of the EM system to magnetite may not match that from a magnetometer survey. First, HEM-derived susceptibility is a rock property measurement, like resistivity. Magnetic data show the total magnetic field, a measure of the potential field, not the rock property. Secondly, the shape of an anomaly depends on the shape and direction of the source magnetic field. The electromagnetic field of HEM is much different in shape from the earth’s magnetic field. Total field magnetic anomalies are different at different magnetic latitudes; HEM susceptibility anomalies have the same shape regardless of their location on the earth.

In far northern latitudes, where the magnetic field is nearly vertical, the total magnetic field measurement over a thin vertical dike is very similar in shape to the anomaly from the HEM-derived susceptibility (a sharp peak over the body). The same vertical dike at the magnetic equator would yield a negative magnetic anomaly, but the HEM susceptibility anomaly would show a positive susceptibility peak.

Effects of Permeability and Dielectric Permittivity

Resistivity algorithms that assume free-space magnetic permeability and dielectric permittivity, do not yield reliable values in highly magnetic or highly resistive areas. Both magnetic polarization and displacement currents cause a decrease in the in-phase component, often resulting in negative values that yield erroneously high apparent resistivities. The effects of magnetite occur at all frequencies, but are most evident at the lowest frequency. Conversely, the negative effects of dielectric permittivity are most evident at the higher frequencies, in resistive areas.

The table below shows the effects of varying permittivity over a resistive (10,000 ohm-m) half space, at frequencies of 56,000 Hz (DIGHEM^V) and 102,000 Hz (RESOLVE).

Apparent Resistivity Calculations
Effects of Permittivity on In-phase/Quadrature/Resistivity

Freq (Hz)	Coil	Sep (m)	Thres (ppm)	Alt (m)	In Phase	Quad Phase	App Res	App Depth (m)	Permittivity
56,000	CP	6.3	0.1	30	7.3	35.3	10118	-1.0	1 Air
56,000	CP	6.3	0.1	30	3.6	36.6	19838	-13.2	5 Quartz
56,000	CP	6.3	0.1	30	-1.1	38.3	81832	-25.7	10 Epidote
56,000	CP	6.3	0.1	30	-10.4	42.3	76620	-25.8	20 Granite
56,000	CP	6.3	0.1	30	-19.7	46.9	71550	-26.0	30 Diabase
56,000	CP	6.3	0.1	30	-28.7	52.0	66787	-26.1	40 Gabbro
102,000	CP	7.86	0.1	30	32.5	117.2	9409	-0.3	1 Air
102,000	CP	7.86	0.1	30	11.7	127.2	25956	-16.8	5 Quartz
102,000	CP	7.86	0.1	30	-14.0	141.6	97064	-26.5	10 Epidote
102,000	CP	7.86	0.1	30	-62.9	176.0	83995	-26.8	20 Granite
102,000	CP	7.86	0.1	30	-107.5	215.8	73320	-27.0	30 Diabase
102,000	CP	7.86	0.1	30	-147.1	259.2	64875	-27.2	40 Gabbro

Methods have been developed (Huang and Fraser, 2000, 2001) to correct apparent resistivities for the effects of permittivity and permeability. The corrected resistivities yield more credible values than if the effects of permittivity and permeability are disregarded.

Recognition of Culture

Cultural responses include all EM anomalies caused by man-made metallic objects. Such anomalies may be caused by inductive coupling or current gathering. The concern of the interpreter is to recognize when an EM response is due to culture. Points of consideration used by the interpreter, when coaxial and coplanar coil-pairs are operated at a common frequency, are as follows:

1. Channels CXPL and CPPL monitor 60 Hz radiation. An anomaly on these channels shows that the conductor is radiating power. Such an indication is normally a guarantee that the conductor is cultural. However, care must be taken to ensure that the conductor is not a geologic body that strikes across a power line, carrying leakage currents.

2. A flight that crosses a "line" (e.g., fence, telephone line, etc.) yields a centre-peaked coaxial anomaly and an m-shaped coplanar anomaly.[7] When the flight crosses the cultural line at a high angle of intersection, the amplitude ratio of coaxial/coplanar response is 2. Such an EM anomaly can only be caused by a line. The geologic body that yields anomalies most closely resembling a line is the vertically dipping thin dike. Such a body, however, yields an amplitude ratio of 1 rather than 2. Consequently, an m-shaped coplanar anomaly with a CXI/CPI amplitude ratio of 2 is virtually a guarantee that the source is a cultural line.

3. A flight that crosses a sphere or horizontal disk yields centre-peaked coaxial and coplanar anomalies with a CXI/CPI amplitude ratio (i.e., coaxial/coplanar) of 1/8. In the absence of geologic bodies of this geometry, the most likely conductor is a metal roof or small fenced yard.[8] Anomalies of this type are virtually certain to be cultural if they occur in an area of culture.

4. A flight that crosses a horizontal rectangular body or wide ribbon yields an m-shaped coaxial anomaly and a centre-peaked coplanar anomaly. In the absence of geologic bodies of this geometry, the most likely conductor is a large fenced area.[5] Anomalies of this type are virtually certain to be cultural if they occur in an area of culture.

5. EM anomalies that coincide with culture, as seen on the camera film or video display, are usually caused by culture. However, care is taken with such coincidences because a geologic conductor could occur beneath a fence, for example. In this example, the fence would be expected to yield an m-shaped coplanar anomaly as in case #2 above. If, instead, a centre-peaked coplanar anomaly occurred, there would be concern that a thick geologic conductor coincided with the cultural line.

6. The above description of anomaly shapes is valid when the culture is not conductively coupled to the environment. In this case, the anomalies arise from inductive coupling to the EM transmitter. However, when the environment is quite conductive (e.g., less than 100 ohm-m at 900 Hz), the cultural conductor may be conductively coupled to the environment. In this latter case, the anomaly shapes tend to be governed by current gathering. Current gathering can completely distort

---

[7] See Figure C-1 presented earlier.

[8] It is a characteristic of EM that geometrically similar anomalies are obtained from: (1) a planar conductor, and (2) a wire which forms a loop having dimensions identical to the perimeter of the equivalent planar conductor.

the anomaly shapes, thereby complicating the identification of cultural anomalies. In such circumstances, the interpreter can only rely on the radiation channels and on the camera film or video records.

Magnetic Responses

The measured total magnetic field provides information on the magnetic properties of the earth materials in the survey area. The information can be used to locate magnetic bodies of direct interest for exploration, and for structural and lithological mapping.

The total magnetic field response reflects the abundance of magnetic material in the source. Magnetite is the most common magnetic mineral. Other minerals such as ilmenite, pyrrhotite, franklinite, chromite, hematite, arsenopyrite, limonite and pyrite are also magnetic, but to a lesser extent than magnetite on average.

In some geological environments, an EM anomaly with magnetic correlation has a greater likelihood of being produced by sulphides than one which is non-magnetic. However, sulphide ore bodies may be non-magnetic (e.g., the Kidd Creek deposit near Timmins, Canada) as well as magnetic (e.g., the Mattabi deposit near Sturgeon Lake, Canada).

Iron ore deposits will be anomalously magnetic in comparison to surrounding rock due to the concentration of iron minerals such as magnetite, ilmenite and hematite.

Changes in magnetic susceptibility often allow rock units to be differentiated based on the total field magnetic response. Geophysical classifications may differ from geological classifications if various magnetite levels exist within one general geological classification. Geometric considerations of the source such as shape, dip and depth, inclination of the earth's field and remanent magnetization will complicate such an analysis.

In general, mafic lithologies contain more magnetite and are therefore more magnetic than many sediments which tend to be weakly magnetic. Metamorphism and alteration can also increase or decrease the magnetization of a rock unit.

Textural differences on a total field magnetic contour, colour or shadow map due to the frequency of activity of the magnetic parameter resulting from inhomogeneities in the distribution of magnetite within the rock, may define certain lithologies. For example, near surface volcanics may display highly complex contour patterns with little line-to-line correlation.

Rock units may be differentiated based on the plan shapes of their total field magnetic responses. Mafic intrusive plugs can appear as isolated "bulls-eye" anomalies. Granitic intrusives appear as sub-circular zones, and may have contrasting rings due to contact metamorphism. Generally, granitic terrain will lack a pronounced strike direction, although granite gneiss may display strike.

Linear north-south units are theoretically not well-defined on total field magnetic maps in equatorial regions due to the low inclination of the earth's magnetic field. However, most stratigraphic units will have variations in composition along strike that will cause the units to appear as a series of alternating magnetic highs and lows.

Faults and shear zones may be characterized by alteration that causes destruction of magnetite (e.g., weathering) that produces a contrast with surrounding rock. Structural breaks may be filled by magnetite-rich, fracture filling material as is the case with diabase dikes, or by non-magnetic felsic material.

Faulting can also be identified by patterns in the magnetic total field contours or colours. Faults and dikes tend to appear as lineaments and often have strike lengths of several kilometres. Offsets in narrow, magnetic, stratigraphic trends also delineate structure. Sharp contrasts in magnetic lithologies may arise due to large displacements along strike-slip or dip-slip faults.

APPENDIX D

FLIGHT LOGS

FUGRO FLIGHT LOG

EM SYSTEM Resolve 3 JOB# 04034 FLT# 40

DATE	Aug 12/04	VIDEO CHK	ON	VIDEO VERIFIED?	YES / NO
OPERATOR	DG	BIRD GPS CHK	ON	LASER ALTIMETER?	(YES) / NO
PILOT	BH	FLIGHT TIME	START:	END:	TOTAL:
WEATHER	TURB:		TEMP:	PRECIP:	SPHERICS:

START	1	2	3	4	5	6
FOP	25K	5183	310	140K	1798	3522
TX	18.7	25.7	24.3	28.7	29.5	19.1
RX						

END	1	2	3	4	5	6
FOP	25K	8151	391	140K	1800	3326
TX	17.5	22.4	21.5	26.5	27.0	17.7
RX	3	11	18	27	20	3

	Line	Dir	Start Fid	End Fid	kms	**DATA ALERT** **NOTES**
Ac Q	10011	N	1940	1740		
Q	10020	S	2220	2805		
	10030	N	2830	3440		around house @ start
Q	10040	S	3715	4305		
	10050	N	4355	4970		around houses @ start 4860 around h.
Q	10060	S	5250	5800		around houses @ end
	10070	N	5905	6525		around houses @ start
Q	10080	S	6790	7440		735 around farm
	10090	N	7470	8075		
Q	10100	S	8335	8975		
	10110	N	9010	9620		around sch. school @ start
Q	10120	S	9895			cut short for school
Q						

Reference GPS:

Mobile GPS:

Base Mag:

EM Levels:

FLIGHT LOG

EM SYSTEM Resolve 3 JOB# 04034 FLT# 41

DATE	Aug 12/04	VIDEO CHK	ON	VIDEO VERIFIED?	YES / NO
OPERATOR	DB	BIRD GPS CHK	ON	LASER ALTIMETER?	YES / NO
PILOT	BH	FLIGHT TIME	START:	END:	TOTAL:
WEATHER	TURB:		TEMP:	PRECIP:	SPHERICS:

START	1	2	3	4	5	6
FOP	25K	5165	391	140K	1501	3330
TX	15.3	23.3	22.6	27.5	28.3	18.6
RX	3	12	19	28	20	3

END	1	2	3	4	5	6
FOP	25K	5150	391	140K	1501	3328
TX	17.3	21.8	21.3	26.3	26.7	17.5
RX	3	11	18	26	18	3

	Line	Dir	Start Fid	End Fid	kms	**DATA ALERT** **NOTES**
AC Q	10130	N	1065	1650		
Q	10140	S	1155	2545		
	10150	N	2590	3175		ground hauses @ start
Q	10160	S	3405	4020		" " @ end
	10170	N	4060	4640		" " @ start
Q	10180	S	4830	5400		
	10190	N	5440	6035		
Q	10200	S	6300	6885		
	10210	N	6925	7465		
Q	10220	S	7680	8260		
	10230	N	8300	8860		
Q	10240	S	9090	9685		
Q						

Reference GPS: _____

Mobile GPS: _____

Base Mag: _____

EM Levels: _____

FUGRO FLIGHT LOG

EM SYSTEM Resolve 3 JOB# 04034 FLT# 42

DATE	Aug 12/04	VIDEO CHK	ON	VIDEO VERIFIED?	YES / NO
OPERATOR	DB	BIRD GPS CHK	ON	LASER ALTIMETER?	YES / NO
PILOT	BH	FLIGHT TIME	START:	END:	TOTAL:
WEATHER	TURB:		TEMP:	PRECIP:	SPHERICS:

START	1	2	3	4	5	6
FOP	25K	8172	391	140K	1802	3331
TX	15.4	23.1	22.7	27.4	25.3	18.6
RX	3	12	19	27	19	3

END	1	2	3	4	5	6
FOP	25K	8148	391	140K	1802	3328
TX	14.2	21.6	21.2	26.1	26.5	12.4
RX	3	11	17	25	18	3

	Line	Dir	Start Fid	End Fid	kms	**DATA ALERT** **NOTES**
AC Q	10250	N	1015	1615		around house @ start
Q	10260	S	1830	2435		
	10270	N	2470	3025		
Q	10280	S	3255	3815		
	10290	N	3850	4395		
Q	10300	S	4610	5185		
	10310	N	5225	5765		
Q	10320	S	5965	6545		
	10330	N	6590	7165		
Q	10340	S	7425	7990		
	10350	N	8040	8595		
Q	10360	S	8780	9315		
Q						

Reference GPS: _____
Mobile GPS: _____
Base Mag: _____

EM Levels: _____

FUGRO FLIGHT LOG

EM SYSTEM R-sol 3 JOB# 04034 FLT# 43

DATE	Aug 13/04	VIDEO CHK	ON	VIDEO VERIFIED?	YES / NO
OPERATOR	DS	BIRD GPS CHK	ON	LASER ALTIMETER?	YES / NO
PILOT	BH	FLIGHT TIME	START:	END:	TOTAL:
WEATHER	TURB:		TEMP:	PRECIP:	SPHERICS:

START	1	2	3	4	5	6
FOP	25K	8183	390	1406	1775	3322
TX	18.7	25.8	24.3	25.7	29.5	19.1
RX	3	14	20	29	20	3

END	1	2	3	4	5	6
FOP	25K	8151	391	1406K	1801	3327
TX	17.5	22.3	21.5	26.5	26.9	17.7
RX	3	12	14	26	15	3

AC

	Line	Dir	Start Fid	End Fid	kms	**DATA ALERT** **NOTES**
Q	10370	N	1840	2390		
Q	10380	S	2625	2210		
	10390	N	3265	3815		
Q	10400	S	4045	4620		
	10410	N	4650	5250		
Q	10420	S	5455	6055		
	10430	N	6110	6700		
Q	10440	S	7000	7585		
	10450	N	7650	8195		
Q	10460	S	8415	8965		
	10470	N	9005	9565		
Q	10480	S	9765	10310		
Q						

Reference GPS: _____ _____

Mobile GPS: _____ _____

Base Mag: _____ _____

_____ _____

EM Levels: _____

FUGRO FLIGHT LOG

EM SYSTEM Resolve 3 JOB# 04034 FLT# 44

DATE	Aug 13/04	VIDEO CHK	ON	VIDEO VERIFIED?	YES / NO
OPERATOR	OB	BIRD GPS CHK	ON	LASER ALTIMETER?	(YES) / NO
PILOT	BH	FLIGHT TIME	START:	END:	TOTAL:
WEATHER	TURB:		TEMP:	PRECIP:	SPHERICS:

START	1	2	3	4	5	6
FOP	25K	5170	391	3140K	1502	3328
TX	18.1	23.2	22.7	27.2	28.1	18.4
RX	3	13	20	27	19	3

END	1	2	3	4	5	6
FOP						
TX						
RX						

	Line	Dir	Start Fid	End Fid	kms	**DATA ALERT** **NOTES**
AC Q	10490	N	1700	2245		
Q	10500	S	2465	3035		
E	10510	N	3050	3600		
Q	10520	S	3830	4375		
	10530	N	4420	4955		
Q	10540	S	5185	5725		
	10550	N	5775	6285	19.9	
Q	10560	S	6500	6915	15.1	
	10570	N	6965	7355		
Q	10580	S	7510	7930		
	10590	N	7975	8380		
	10600	S	8435	8865		
Q						

Reference GPS: _____

Mobile GPS: _____

Base Mag: _____

EM Levels: _____

196.3 + 29.3 =

226.3
22

FLIGHT LOG

EM SYSTEM Resolve 3 JOB# 04034 FLT# 45

DATE	Aug 13/04	VIDEO CHK	ON	VIDEO VERIFIED?	(YES) NO
OPERATOR	DB	BIRD GPS CHK	ON	LASER ALTIMETER?	(YES) NO
PILOT	BH	FLIGHT TIME	START:	END:	TOTAL:
WEATHER	TURB: Moderate		TEMP:	PRECIP:	SPHERICS:

START	1	2	3	4	5	6
FOP	25K	5170	391	140K	1803	3331
TX	18.3	22.7	22.2	27.3	28.0	18.3
RX	3	12	19	27	19	3
END	**1**	**2**	**3**	**4**	**5**	**6**
FOP	25K	5147	391	140K	1802	3330
TX	12.1	21.3	21.0	25.8	26.3	17.2
RX	3	11	17	26	18	3

	Line	Dir	Start Fid	End Fid	kms	**DATA ALERT** **NOTES**
AC Q	19010	E	1105			
Q	10610	S	1745	2190		
	10620	N	2235	2660		
	10630	S	2755	3170		
Q	10640	N	3375	3775		
	10650	S	3825	4250		
	10660	N	4315	4725		
Q	10670	S	4905	5325		
	10680	N	5390	5810		
	10690	S	5860	6270		
Q	10700	N	6470	6885		
	10710	S	6930	7355		
	10720	N	7405	7815		
Q	10730	S	8010	8445		
	19020	W	8640	9030		
Q						

Reference GPS: _____
Mobile GPS: _____
_____
Base Mag: _____
_____

EM Levels: _____
_____
_____
_____
_____

139.2

FUGRO FLIGHT LOG

EM SYSTEM Resolve3 JOB# 04034 FLT# 46

DATE	Aug 14/04	VIDEO CHK	ON	VIDEO VERIFIED?	YES / NO
OPERATOR	DB	BIRD GPS CHK	ON	LASER ALTIMETER?	(YES) / NO
PILOT	BH	FLIGHT TIME	START:	END:	TOTAL:
WEATHER	TURB:		TEMP:	PRECIP:	SPHERICS:

START	1	2	3	4	5	6
FOP	25K	5183	3900	14ØK	18ØØ	3325
TX	18.6	25.2	24.3	28.4	29.4	19.Ø
RX	3	14	21	28	2Ø	3

END	1	2	3	4	5	6
FOP	25K	8147	391	14ØK	1802	3328
TX	17.2	21.6	21.2	26.Ø	26.5	17.3
RX	3	11	18	25	18	3

	Line	Dir	Start Fid	End Fid	kms	**DATA ALERT** **NOTES**
A	200210	N	1535	1685	4.8	Infill Block #1
	200230	S	1755	1915		
	200240	N	1950	2135		
	200250	S	2200	2375		
	200260	N	2440	2595		
Q	200280	S	2840	3010		
	201000	N	3065	3225		
	201220	S	3300	3465		
	201400	N	3535	3685		
	201600	S	3750	3905		
	201800	N	3965	4125		
Q	202000	S	4325	4485		
	202200	N	4555	4700		
	202400	S	4765	4930		
	202500	N	4990	5140		
	202460	S	5250	5405		over powerline
	202450	N	5460	5610		
Q	202440	S	5810	5970		
	202430	N	6030	6175		
	202420	S	6240	6400		
	202400	N	6460	6605		
	202380	S	6670	6535		
	202360	N	6885	7040		
Q	202340	S	7290	7450		
	202320	N	7515	7660		
	202300	S	7720	7885		
	202280	N	7935	8085		
	202270	S	8150	8315		
	202260	N	8370	8515	4.8	
Q	202340	S	8830	9090		Infill block #2

-> (over)

Reference GPS: _____ EM Levels: _____

Mobile GPS: _____

Base Mag: _____

171.2

INFILL 2 = 136
INFILL 1 = 111

FLIGHT 46 CONTINUED

Line	Dir	Start Fid	End Fid	kms	**DATA ALERT** **NOTES**
20330	N	9165	9395	8.0	
20320	S	9450	9705		
20310	N	9760	10000		

1368.
29.3

TOTAL=

FLIGHT LOG

EM SYSTEM Resolve 3 JOB# 04034 FLT# 47

DATE	Aug 14/01	VIDEO CHK		VIDEO VERIFIED?	YES / NO
OPERATOR	OG	BIRD GPS CHK	ON	LASER ALTIMETER?	(YES) NO
PILOT	BH	FLIGHT TIME	START:	END:	TOTAL:
WEATHER	TURB: moderate		TEMP:	PRECIP:	SPHERICS:

START	1	2	3	4	5	6
FOP	25K	8157	391	140K	1802	3330
TX	17.6	32.0	21.8	26.4	27.2	17.8
RX						

END	1	2	3	4	5	6
FOP						
TX						
RX						

	Line	Dir	Start Fid	End Fid	kms	**DATA ALERT** **NOTES**
AC Q	20300	N	1180	1400		
	20280	S	1455	1725		
	20260	N	1805	2030		
Q	20240	S	2255	2500		
Q	20220	N	2555	2785		
	20200	S	2860	3115		
	20190	N	3165	3390		
Q	20180	S	3595	3845		over PL
	20170	N	3910	4140		
	20160	S	4205	4480		over PL
	20140	N	4540	4770		
Q	20120	S	4990	5240		
	20100	N	5300	5530		
	20080	S	5590	5845		
	20060	N	5900	6130		
Q	20050	S	6330	6580		
	20040	N	6655	6900		
	20020	S	6955	7200		
Q	20020	N	7280	7510		

Reference GPS: _____
Mobile GPS: _____

Base Mag: _____

EM Levels: _____

Appendix E – Tests and Calibrations

Altimeter Test – Performed August 2, 2004

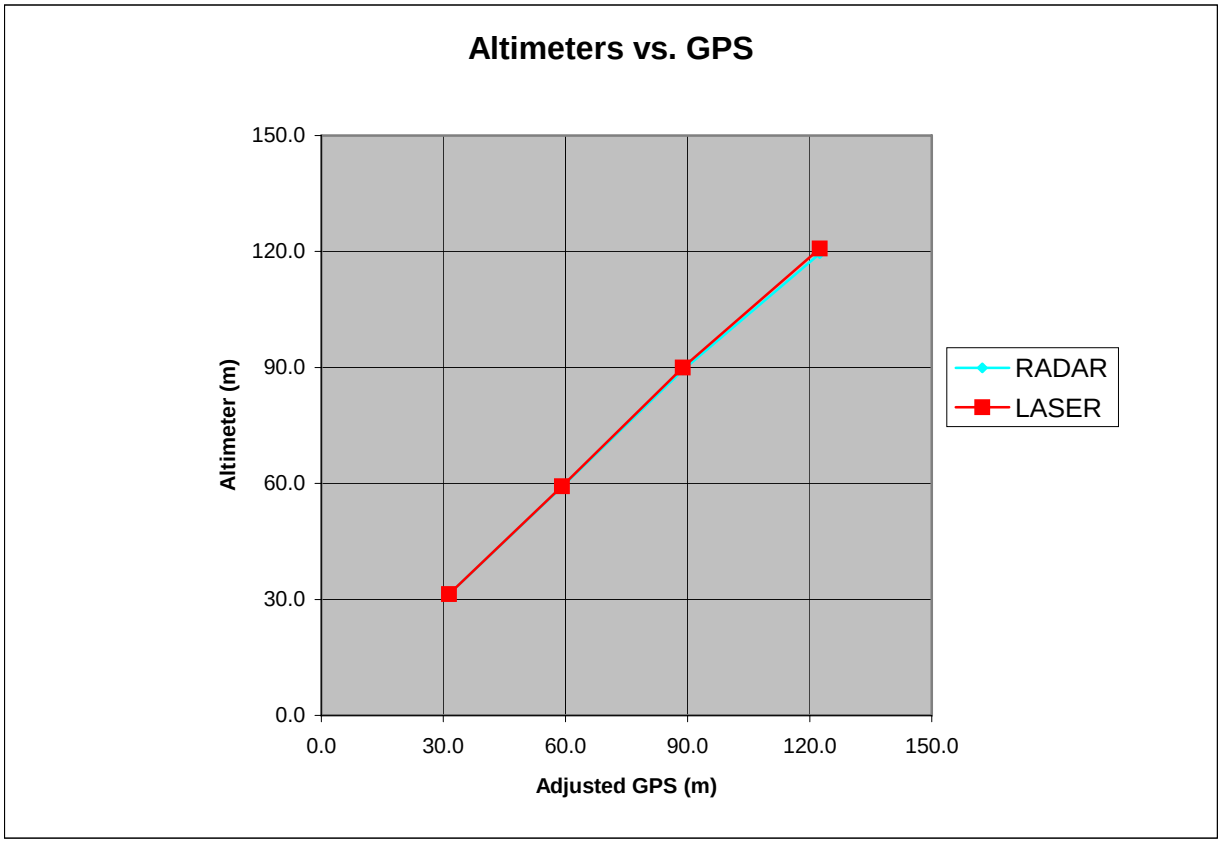

-GPS data zeroed at the first point to match radar and laser data
-radar data has 27.7 metres removed from raw to represent bird altitude.

Results of Altimeter Test including EM data

TARGET (m)	RADAR (m)	LASER (m)	GPS (m)	GPS0 (m)	L140I (ppm)	L140Q (ppm)	L40KI (ppm)	L40KQ (ppm)	L8K2I (ppm)	L8K2Q (ppm)	L1K8I (ppm)	L1K8Q (ppm)	L400I (ppm)	L400Q (ppm)	L3X3I (ppm)	L3X3Q (ppm)
30	31.4	31.4	1399.4	31.4	3002.3	486.4	2319.4	689.3	1212.4	907.9	636.5	740.4	141.7	314.9	314.0	300.6
60	59.1	59.2	1427.1	59.2	519.7	53.5	418.8	80.2	281.9	138.7	201.1	151.1	63.8	95.0	89.5	57.4
90	89.3	90.0	1456.8	88.8	156.7	13.5	124.6	21.9	93.0	38.2	75.0	43.0	31.4	38.2	31.7	17.0
120	119.5	120.8	1490.5	122.5	70.0	7.6	55.3	9.7	40.6	19.8	30.7	18.3	15.6	19.3	14.1	8.8

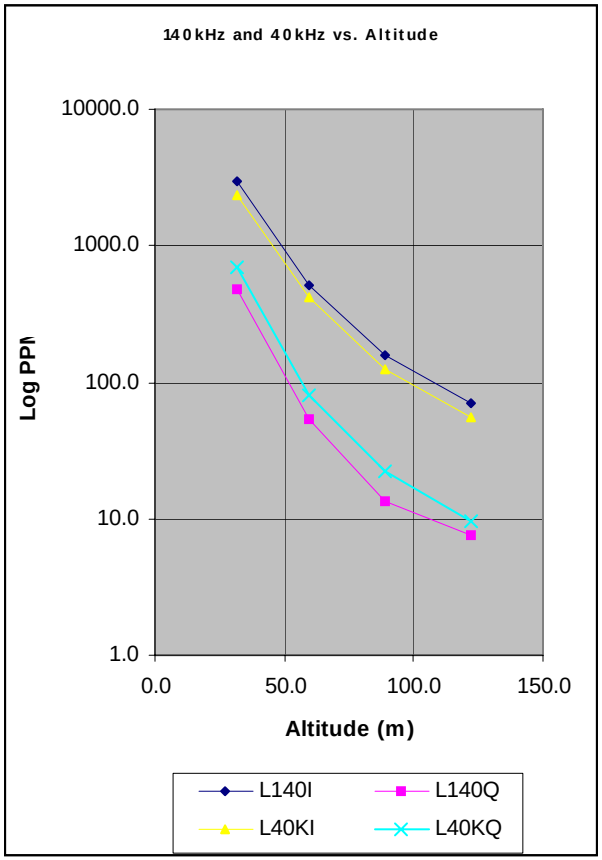

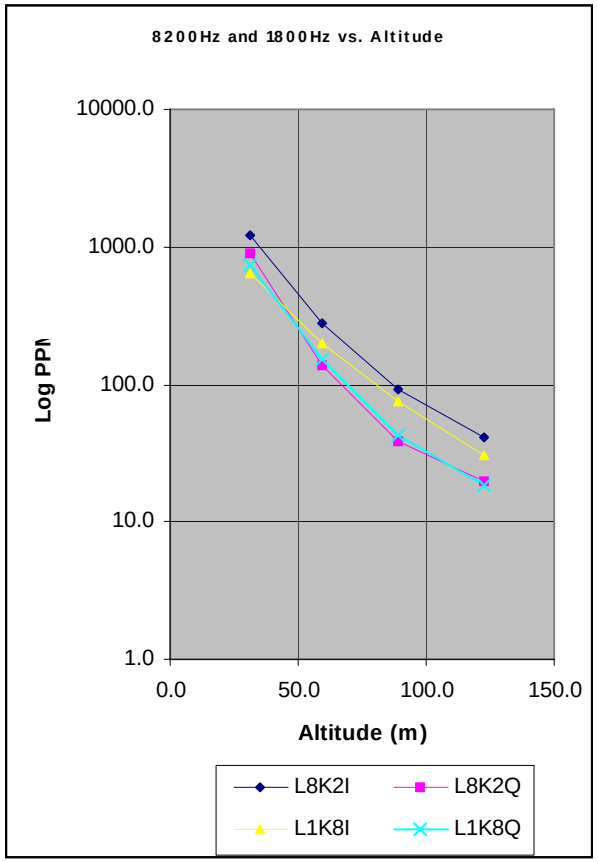

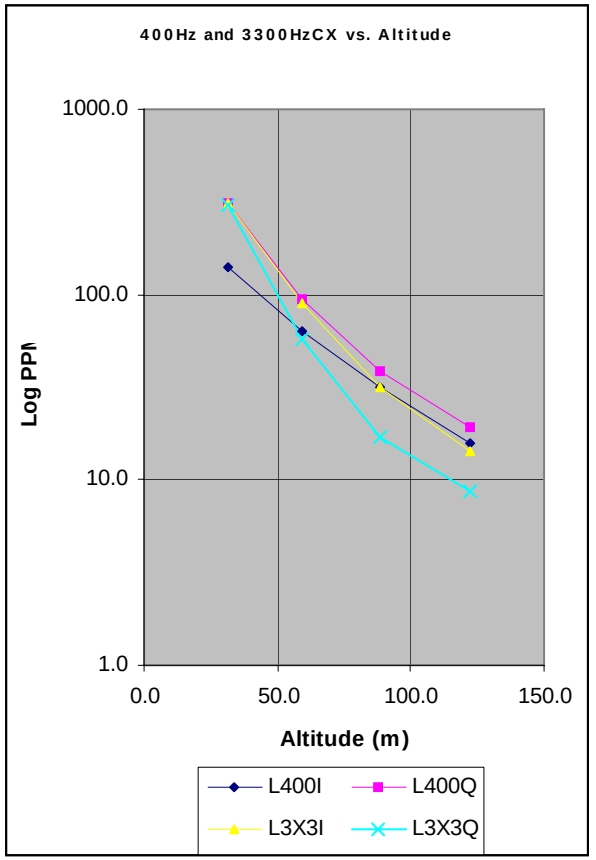

- All data channels averaged over a 50 second period with altitude variation of less than 5 metres
- GPS0 channel is GPS adjusted to first radar/laser value

EM Calibrations

CALIBRATION OF THE DIGHEM DIGITAL (DSP) SYSTEM

The calibration method used in the digital Dighem^{V} has been developed as a significant improvement over the practices described by Fitterman (1998), which practices were originally developed through experimentation and consultation between Fugro and the United States Geological Survey. The problems defined by Fitterman, including jig calibration and conductive ground response, are obviated by calibration at high altitude using internal, rigidly mounted, automatically triggered and measured calibration coils.

Calibration of the system during the survey will use the Fugro AutoCal™ automatic, internal calibration process. At the beginning and end of each flight, and at intervals during the flight, the system will be flown up to high altitude to remove it from any "ground effect" (response from the earth). Any remaining signal from the receiver coils (base level) will be measured as the zero level, and removed from the data collected until the time of the next calibration. Following the zero level setting, internal calibration coils, for which the response phase and amplitude have been determined at the factory, are automatically triggered – one for each frequency. The on-time of the coils is sufficient to determine an accurate response through any ambient noise. The receiver response to each calibration coil "event" is compared to the expected response (from the factory calibration) for both phase angle and amplitude, and the applied phase and gain corrections adjusted to bring the data to the correct value.

In addition, the output of the transmitter coils are continuously monitored during the survey, and the applied gains adjusted to correct for any change in transmitter output (due to heating, etc.)

Because the internal calibration coils are calibrated at the factory (on a resistive halfspace) ground calibrations using external calibration coils on-site are not necessary for system calibration. A check calibration may be carried out on-site to ensure all systems are working correctly. All system calibrations will be carried out in the air, at sufficient altitude that there will be no measurable response from the ground.

The internal calibration coils are rigidly positioned and mounted in the system relative to the transmitter and receiver coils. In addition, when the internal calibration coils are calibrated at the factory, a rigid jig is employed to ensure accurate response from the external coils.

Using real time Fast Fourier Transforms and the calibration procedures outlined above, the data will be processed in real time from measured total field at a high sampling rate to in-phase and quadrature values at 10 samples per second.

Greg Hodges, Chief Geophysicist 01/04/09

References:
Fitterman, D.V., (1998). Sources of calibration errors in helicopter EM data. Exploration Geophysics 29, 65-70.

External Calibration Results

Aug. 2, 2004 Start calibration. Burger Draw, Wyoming

FREQUENCY	CHANNEL	INTERNAL		EXTERNAL		PHASE
		MEASURED	TARGET	MEASURED	TARGET	(degrees)
400	L400I	207	210	199	200.4	0.1
(391)	L400Q	209	210	198	200.4	
1800	L1K8I	201	196	194	204.2	-0.5
(1801)	L1K8Q	201	196	201	204.2	
3300	L3X3I	82	89	101	99.9	1.7
(3326)	L3X3Q	83	89	102	99.9	
8200	L8K2I	156	157	180	207.5	2.8
(8162)	L8K2Q	164	157	197	207.5	
40000	L40KI	558	580	148	192.5	3.4
(39130)	L40KQ	572	580	183	192.5	
140000	L140I	810	787	154	178.8	3.4
(132640)	L140Q	815	787	186	178.8	

Sep. 3, 2004 End calibration. At Fugro's calibrations site, Mountsburg, Ontario

FREQUENCY	CHANNEL	INTERNAL		EXTERNAL		PHASE
		MEASURED	TARGET	MEASURED	TARGET	(degrees)
400	L400I	210	210	201	200.4	0.4
(391)	L400Q	209	210	201	200.4	
1800	L1K8I	194	196	205	204.2	0.2
(1801)	L1K8Q	196	196	206	204.2	
3300	L3X3I	88	89	101	99.9	0.7
(3326)	L3X3Q	88	89	103	99.9	
8200	L8K2I	157	157	208	207.5	-0.2
(8162)	L8K2Q	158	157	203	207.5	
40000	L40KI	579	580	192	192.5	0.8
(39130)	L40KQ	578	580	192	192.5	
140000	L140I	778	787	176	178.8	0.4
(132640)	L140Q	777	787	178	178.8	

-Phase calculated from inverse TAN of quad deflection/inphase deflection.
-Variations in phase and gain values attributed to temperature and location changes for each calibration.

Appendix F - Processing Log

Total Magnetic Field data

A fourth difference was calculated from the raw total magnetic intensity data (TMI). The raw TMI was examined in profile form along with the fourth difference. Spikes and duplicate points were manually defaulted and interpolated with an Akima spline. None of the defaulted areas exceeded one second in length. The diurnal variations recorded by the base station were edited for any cultural contamination and filtered to remove high-frequency noise. This diurnal magnetic data was then subtracted from the despiked TMI to provide a first order diurnal correction. An average base value of 57352 nT was added back to the diurnal corrected airborne total magnetic field records. The diurnal removed magnetic field data were then gridded and compared to a grid of the despiked magnetic data to ensure that the data quality was improved by diurnal removal.

The lag in the magnetic data was determined to be –1.5 seconds and was applied to the survey data. A vertical gradient was calculated from the lagged magnetic data and examined for evidence of leveling and additional lag problems. The IGRF was calculated using the latest coefficient set for the survey date with the altitude taken from the differentially corrected height above the WGS84 spheroid. To remove any short wavelength residual line-to-line discrepancies in the total magnetic field, a microleveling technique was used to remove errors of less than 2.0 nT striking parallel to the line direction. Vertical gradient grids were recalculated from the magnetic grids after each leveling correction. These grids were shadowed and examined to determine the success of the manual correction. This microleveled channel was used to produce the final residual magnetic field grid.

Electromagnetic and Resistivity data

Base level corrections were picked at each high altitude background. These level picks were applied to the raw EM data which were then loaded into the Geosoft database. An 11-point median filter followed by an 11-point Hanning filter was applied to the raw base leveled data. Apparent resistivity and depth calculations were done on the filtered, base leveled EM data using Fugro's proprietary resistivity algorithm. All in-phase, quadrature and resistivity channels were gridded and examined, and manual leveling corrections and phase adjustments were applied as required. The resistivity calculation and gridding was repeated until no further corrections were required. Additional algorithms were run on the data to determine the centroid depths, differential resistivity and differential depths. Sengpiel-type and differential resistivity depth sections were generated to double check the resistivity leveling.

Two sets of grids were generated. The 100 metre spaced detail area was windowed out of the block and gridded with 20 metre cells (1/5 of the line spacing). The remaining area flown at 200-metre spacing was gridded using 40 metre cells. A grid function was run on the 40 metre grids to reduce the cell size to 20 metres and the two grids were merged together, averaging the grid values in a 2 cell overlap. The merged grids were then filtered for final presentation using the following rectangular Hanning filter values:

RES115K	3x3
RES25K	3x3
RES6200	3x3
RES1500	5x5
RES400	5x5

Appendix G - GLOSSARY OF AIRBORNE GEOPHYSICAL TERMS

Note: The definitions given in this glossary refer to the common terminology as used in airborne geophysics.

altitude attenuation: the absorption of gamma rays by the atmosphere between the earth and the detector. The number of gamma rays detected by a system decreases as the altitude increases.

apparent- : the ***physical parameters*** of the earth measured by a geophysical system are normally expressed as apparent, as in "apparent ***resistivity*****"**. This means that the measurement is limited by assumptions made about the geology in calculating the response measured by the geophysical system. Apparent resistivity calculated with ***HEM***, for example, generally assumes that the earth is a ***homogeneous half-space*** – not layered.

amplitude: The strength of the total electromagnetic field. In ***frequency domain*** it is most often the sum of the squares of ***in-phase*** and ***quadrature*** components. In multi-component electromagnetic surveys it is generally the sum of the squares of all three directional components.

analytic signal: The total amplitude of all the directions of magnetic ***gradient***. Calculated as the sum of the squares.

anisotropy: Having different ***physical parameters*** in different directions. This can be caused by layering or fabric in the geology. Note that a unit can be anisotropic, but still **homogeneous**.

anomaly: A localized change in the geophysical data characteristic of a discrete source, such as a conductive or magnetic body. Something locally different from the **background**.

B-field: In time-domain **electromagnetic** surveys, the magnetic field component of the (electromagnetic) **field**. This can be measured directly, although more commonly it is calculated by integrating the time rate of change of the magnetic field **dB/dt**, as measured with a receiver coil.

background: The "normal" response in the geophysical data – that response observed over most of the survey area. **Anomalies** are usually measured relative to the background. In airborne gamma-ray spectrometric surveys the term defines the **cosmic**, radon, and aircraft responses in the absence of a signal from the ground.

base-level: The measured values in a geophysical system in the absence of any outside signal. All geophysical data are measured relative to the system base level.

base frequency: The frequency of the pulse repetition for a ***time-domain electromagnetic*** system. Measured between subsequent positive pulses.

bird: A common name for the pod towed beneath or behind an aircraft, carrying the geophysical sensor array.

calibration coil: A wire coil of known size and dipole moment, which is used to generate a field of known ***amplitude*** and ***phase*** in the receiver, for system calibration. Calibration coils can be external, or internal to the system. Internal coils may be called Q-coils.

coaxial coils: **[CX]** Coaxial coils are in the vertical plane, with their axes horizontal and collinear in the flight direction. These are most sensitive to vertical conductive objects in the ground, such as thin, steeply dipping conductors perpendicular to the flight direction. Coaxial coils generally give the sharpest anomalies over localized conductors. (See also ***coplanar coils***)

coil: A multi-turn wire loop used to transmit or detect electromagnetic fields. Time varying ***electromagnetic*** fields through a coil induce a voltage proportional to the strength of the field and the rate of change over time.

compensation: Correction of airborne geophysical data for the changing effect of the aircraft. This process is generally used to correct data in ***fixed-wing time-domain electromagnetic*** surveys (where the transmitter is on the aircraft and the receiver is moving), and magnetic surveys (where the sensor is on the aircraft, turning in the earth's magnetic field.

component: In ***frequency domain electromagnetic*** surveys this is one of the two **phase** measurements – ***in-phase or quadrature***. In "multi-component" electromagnetic surveys it is also used to define the measurement in one geometric direction (vertical, horizontal in-line and horizontal transverse – the Z, X and Y components).

Compton scattering: gamma ray photons will bounce off the nuclei of atoms they pass through (earth and atmosphere), reducing their energy and then being detected by ***radiometric*** sensors at lower energy levels. See also ***stripping***.

conductance: See ***conductivity thickness***

conductivity: [σ] The facility with which the earth or a geological formation conducts electricity. Conductivity is usually measured in milli-Siemens per metre (mS/m). It is the reciprocal of ***resistivity***.

conductivity-depth imaging: see ***conductivity-depth transform***.

conductivity-depth transform: A process for converting electromagnetic measurements to an approximation of the conductivity distribution vertically in the earth, assuming a ***layered earth***. (Macnae and Lamontagne, 1987; Wolfgram and Karlik, 1995)

conductivity thickness: [σ**t**] The product of the ***conductivity***, and thickness of a large, tabular body. (It is also called the "conductivity-thickness product") In electromagnetic geophysics, the response of a thin plate-like conductor is proportional to the conductivity multiplied by thickness. For example a 10 metre thickness of 20 Siemens/m

mineralization will be equivalent to 5 metres of 40 S/m; both have 200 S conductivity thickness. Sometimes referred to as conductance.

conductor: Used to describe anything in the ground more conductive than the surrounding geology. Conductors are most often clays or graphite, or hopefully some type of mineralization, but may also be man-made objects, such as fences or pipelines.

coplanar coils: **[CP]** The coplanar coils lie in the horizontal plane with their axes vertical, and parallel. These coils are most sensitive to massive conductive bodies, horizontal layers, and the ***halfspace***.

cosmic ray: High energy sub-atomic particles from outer space that collide with the earth's atmosphere to produce a shower of gamma rays (and other particles) at high energies.

counts (per second): The number of ***gamma-rays*** detected by a gamma-ray ***spectrometer*.** The rate depends on the geology, but also on the size and sensitivity of the detector.

culture: A term commonly used to denote any man-made object that creates a geophysical anomaly. Includes, but not limited to, power lines, pipelines, fences, and buildings.

current gathering: The tendency of electrical currents in the ground to channel into a conductive formation. This is particularly noticeable at higher frequencies or early time channels when the formation is long and parallel to the direction of current flow. This tends to enhance anomalies relative to inductive currents (see also ***induction***). Also known as current channelling.

current channelling: See current gathering.

daughter products: The radioactive natural sources of gamma-rays decay from the original element (commonly potassium, uranium, and thorium) to one or more lower-energy elements. Some of these lower energy elements are also radioactive and decay further. ***Gamma-ray spectrometry*** surveys may measure the gamma rays given off by the original element or by the decay of the daughter products.

dB/dt: As the ***secondary electromagnetic field*** changes with time, the magnetic field [**B**] component induces a voltage in the receiving ***coil***, which is proportional to the rate of change of the magnetic field over time.

decay: In ***time-domain electromagnetic*** theory, the weakening over time of the ***eddy currents*** in the ground, and hence the ***secondary field*** after the ***primary field*** electromagnetic pulse is turned off. In ***gamma-ray spectrometry***, the radioactive breakdown of an element, generally potassium, uranium, thorium, or one of their ***daughter*** products.

decay series: In ***gamma-ray spectrometry***, a series of progressively lower energy ***daughter products*** produced by the radioactive breakdown of uranium or thorium.

decay constant: see time constant.

depth of exploration: The maximum depth at which the geophysical system can detect the target. The depth of exploration depends very strongly on the type and size of the target, the contrast of the target with the surrounding geology, the homogeneity of the surrounding geology, and the type of geophysical system. One measure of the maximum depth of exploration for an electromagnetic system is the depth at which it can detect the strongest conductive target – generally a highly conductive horizontal layer.

differential resistivity: A process of transforming ***apparent resistivity*** to an approximation of layer resistivity at each depth. The method uses multi-frequency HEM data and approximates the effect of shallow layer ***conductance*** determined from higher frequencies to estimate the deeper conductivities (Huang and Fraser, 1996)

dipole moment: [NIA] For a transmitter, the product of the area of a ***coil***, the number of turns of wire, and the current flowing in the coil. At a distance significantly larger than the size of the coil, the magnetic field from a coil will be the same if the dipole moment product is the same. For a receiver coil, this is the product of the area and the number of turns. The sensitivity to a magnetic field (assuming the source is far away) will be the same if the dipole moment is the same.

diurnal: The daily variation in a natural field, normally used to describe the natural fluctuations (over hours and days) of the earth's magnetic field.

dielectric permittivity: **[ε]** The capacity of a material to store electrical charge, this is most often measured as the relative permittivity [ε_r], or ratio of the material dielectric to that of free space. The effect of high permittivity may be seen in HEM data at high frequencies over highly resistive geology as a reduced or negative ***in-phase***, and higher ***quadrature*** data.

drift: Long-time variations in the base-level or calibration of an instrument.

eddy currents: The electrical currents induced in the ground, or other conductors, by a time-varying ***electromagnetic field*** (usually the ***primary field***). Eddy currents are also induced in the aircraft's metal frame and skin; a source of ***noise*** in EM surveys.

electromagnetic: **[EM]** Comprised of a time-varying electrical and magnetic field. Radio waves are common electromagnetic fields. In geophysics, an electromagnetic system is one which transmits a time-varying ***primary field*** to induce ***eddy currents*** in the ground, and then measures the ***secondary field*** emitted by those eddy currents.

energy window: A broad spectrum of ***gamma-ray*** energies measured by a spectrometric survey. The energy of each gamma-ray is measured and divided up into numerous discrete energy levels, called windows.

equivalent (thorium or uranium): The amount of radioelement calculated to be present, based on the gamma-rays measured from a **daughter** element. This assumes that the ***decay series*** is in equilibrium – progressing normally.

fiducial, or fid: Timing mark on a survey record. Originally these were timing marks on a profile or film; now the term is generally used to describe 1-second interval timing records in digital data, and on maps or profiles.

fixed-wing: Aircraft with wings, as opposed to "rotary wing" helicopters.

footprint: This is a measure of the area of sensitivity under the aircraft of an airborne geophysical system. The footprint of an ***electromagnetic*** system is dependent on the altitude of the system, the orientation of the transmitter and receiver and the separation between the receiver and transmitter, and the conductivity of the ground. The footprint of a ***gamma-ray spectrometer*** depends mostly on the altitude. For all geophysical systems, the footprint also depends on the strength of the contrasting ***anomaly***.

frequency domain: An ***electromagnetic*** system which transmits a ***primary field*** that oscillates smoothly over time (sinusoidal), inducing a similarly varying electrical current in the ground. These systems generally measure the changes in the ***amplitude*** and ***phase*** of the ***secondary field*** from the ground at different frequencies by measuring the **in-phase** and **quadrature** phase components. See also ***time-domain***.

full-stream data: Data collected and recorded continuously at the highest possible sampling rate. Normal data are stacked (see ***stacking***) over some time interval before recording.

gamma-ray: A very high-energy photon, emitted from the nucleus of an atom as it undergoes a change in energy levels.

gamma-ray spectrometry: Measurement of the number and energy of natural (and sometimes man-made) gamma-rays across a range of photon energies.

gradient: In magnetic surveys, the gradient is the change of the magnetic field over a distance, either vertically or horizontally in either of two directions. Gradient data is often measured, or calculated from the total magnetic field data because it changes more quickly over distance than the ***total magnetic field***, and so may provide a more precise measure of the location of a source. See also ***analytic signal***.

ground effect: The response from the earth. A common calibration procedure in many geophysical surveys is to fly to altitude high enough to be beyond any measurable response from the ground, and there establish ***base levels*** or ***backgrounds***.

half-space: A mathematical model used to describe the earth – as infinite in width, length, and depth below the surface. The most common halfspace models are ***homogeneous*** and ***layered earth***.

heading error: A slight change in the magnetic field measured when flying in opposite directions.

HEM: Helicopter ElectroMagnetic, This designation is most commonly used to helicopter-borne, ***frequency-domain*** electromagnetic systems. At present, the transmitter and receivers are normally mounted in a ***bird*** carried on a sling line beneath the helicopter.

herringbone pattern: a pattern created in geophysical data by an asymmetric system, where the **anomaly** may be extended to either side of the source, in the direction of flight. Appears like fish bones, or like the teeth of a comb, extending either side of centre, each tooth an alternate flight line.

homogeneous: This is a geological unit that has the same ***physical parameters*** throughout its volume. This unit will create the same response to an HEM system anywhere, and the HEM system will measure the same apparent ***resistivity*** anywhere. The response may change with system direction (see ***anisotropy***).

in-phase: the component of the measured ***secondary field*** that has the same phase as the transmitter and the ***primary field***. The in-phase component is stronger than the ***quadrature*** phase over relatively higher ***conductivity***.

induction: Any time-varying electromagnetic field will induce (cause) electrical currents to flow in any object with non-zero ***conductivity***. (see ***eddy currents***)

infinite: In geophysical terms, an "infinite' dimension is one much greater than the ***footprint*** of the system, so that the system does not detect changes at the edges of the object.

International Geomagnetic Reference Field: **[IGRF]** An approximation of the smooth magnetic field of the earth, in the absence of variations due to local geology. Once the IGRF is subtracted from the measured magnetic total field data, any remaining variations are assumed to be due to local geology. The IGRF also predicts the slow changes of the field up to five years in the future.

inversion, or **inverse modeling**: A process of converting geophysical data to an earth model, which compares theoretical models of the response of the earth to the data measured, and refines the model until the response closely fits the measured data (Huang and Palacky, 1991)

layered earth: A common geophysical model which assumes that the earth is horizontally layered – the ***physical parameters*** are constant to ***infinite*** distance horizontally, but change vertically.

magnetic permeability: **[μ]** This is defined as the ratio of magnetic induction to the inducing magnetic field. The relative magnetic permeability [μ_r] is often quoted, which is the ratio of the rock permeability to the permeability of free space. In geology and geophysics, the ***magnetic susceptibility*** is more commonly used to describe rocks.

magnetic susceptibility: **[k]** A measure of the degree to which a body is magnetized. In SI units this is related to relative ***magnetic permeability*** by $k=\mu_r-1$, and is a dimensionless unit. For most geological material, susceptibility is influenced primarily by the percentage of magnetite. It is most often quoted in units of 10^{-6}. In HEM data this is most often apparent as a negative ***in-phase*** component over high susceptibility, high ***resistivity*** geology such as diabase dikes.

noise: That part of a geophysical measurement that the user does not want. Typically this includes electronic interference from the system, the atmosphere (***sferics***), and man-made sources. This can be a subjective judgment, as it may include the response from geology other than the target of interest. Commonly the term is used to refer to high frequency (short period) interference. See also ***drift***.

Occam's inversion: an ***inversion*** process that matches the measured ***electromagnetic*** data to a theoretical model of many, thin layers with constant thickness and varying resistivity (Constable et al, 1987).

off-time: In a ***time-domain electromagnetic*** survey, the time after the end of the ***primary field pulse***, and before the start of the next pulse.

on-time: In a ***time-domain electromagnetic*** survey, the time during the ***primary field pulse***.

phase: The angular difference in time between a measured sinusoidal electromagnetic field and a reference – normally the primary field. The phase is calculated from $\tan^{-1}$(***in-phase*** / ***quadrature***).

physical parameters: These are the characteristics of a geological unit. For electromagnetic surveys, the important parameters for electromagnetic surveys are ***conductivity***, ***magnetic permeability*** (or ***susceptibility***) and ***dielectric permittivity***; for magnetic surveys the parameter is magnetic susceptibility, and for gamma ray spectrometric surveys it is the concentration of the major radioactive elements: potassium, uranium, and thorium.

permittivity: see ***dielectric permittivity***.

permeability: see ***magnetic permeability***.

primary field: the EM field emitted by a transmitter. This field induces ***eddy currents*** in (energizes) the conductors in the ground, which then create their own ***secondary fields***.

pulse: In time-domain EM surveys, the short period of intense ***primary*** field transmission. Most measurements (the ***off-time***) are measured after the pulse.

quadrature: that component of the measured ***secondary field*** that is phase-shifted 90° from the ***primary field***. The quadrature component tends to be stronger than the ***in-phase*** over relatively weaker ***conductivity***.

Q-coils: see ***calibration coil***.

radiometric: Commonly used to refer to ***gamma ray*** spectrometry.

radon: A radioactive daughter product of uranium and thorium, radon is a gas which can leak into the atmosphere, adding to the non-geological background of a gamma-ray spectrometric survey.

resistivity: **[ρ]** The strength with which the earth or a geological formation resists the flow of electricity, typically the flow induced by the ***primary field*** of the electromagnetic transmitter. Normally expressed in ohm-metres, it is the reciprocal of ***conductivity***.

resistivity-depth transforms: similar to ***conductivity depth transforms***, but the calculated ***conductivity*** has been converted to ***resistivity***.

resistivity section: an approximate vertical section of the resistivity of the layers in the earth. The resistivities can be derived from the ***apparent resistivity***, the ***differential resistivities***, ***resistivity-depth transforms***, or ***inversions***.

secondary field: The field created by conductors in the ground, as a result of electrical currents induced by the ***primary field*** from the ***electromagnetic*** transmitter. Airborne ***electromagnetic*** systems are designed to create, and measure a secondary field.

Sengpiel section: a ***resistivity section*** derived using the ***apparent resistivity*** and an approximation of the depth of maximum sensitivity for each frequency.

sferic: Lightning, or the ***electromagnetic*** signal from lightning, it is an abbreviation of "atmospheric discharge". These appear to magnetic and electromagnetic sensors as sharp "spikes" in the data. Under some conditions lightning storms can be detected from hundreds of kilometres away. (see ***noise***)

signal: That component of a measurement that the user wants to see – the response from the targets, from the earth, etc. (See also ***noise***)

skin depth: A measure of the depth of penetration of an electromagnetic field into a material. It is defined as the depth at which the primary field decreases to 1/e of the field at the surface. It is calculated by approximately 503 x √(resistivity/frequency). Note that depth of penetration is greater at higher ***resistivity*** and/or lower ***frequency***.

spectrometry: Measurement across a range of energies, where ***amplitude*** and energy are defined for each measurement. In gamma-ray spectrometry, the number of gamma rays are measured for each energy ***window***, to define the ***spectrum***.

spectrum: In ***gamma ray spectrometry***, the continuous range of energy over which gamma rays are measured. In ***time-domain electromagnetic*** surveys, the spectrum is the energy of the **pulse** distributed across an equivalent, continuous range of frequencies.

spheric: see ***sferic***.

stacking: Summing repeat measurements over time to enhance the repeating ***signal***, and minimize the random ***noise***.

stripping: Estimation and correction for the gamma ray photons of higher and lower energy that are observed in a particular ***energy window***. See also ***Compton scattering***.

susceptibility: See ***magnetic susceptibility***.

tau: [τ] Often used as a name for the ***time constant***.

TDEM: ***time domain electromagnetic***.

thin sheet: A standard model for electromagnetic geophysical theory. It is usually defined as thin, flat-lying, and ***infinite*** in both horizontal directions. (see also ***vertical plate***)

tie-line: A survey line flown across most of the ***traverse lines***, generally perpendicular to them, to assist in measuring ***drift*** and ***diurnal*** variation. In the short time required to fly a tie-line it is assumed that the drift and/or diurnal will be minimal, or at least changing at a constant rate.

time constant: The time required for an ***electromagnetic*** field to decay to a value of 1/e of the original value. In ***time-domain*** electromagnetic data, the time constant is proportional to the size and ***conductance*** of a tabular conductive body. Also called the decay constant.

Time channel: In ***time-domain electromagnetic*** surveys the decaying ***secondary field*** is measured over a period of time, and the divided up into a series of consecutive discrete measurements over that time.

time-domain: ***Electromagnetic*** system which transmits a pulsed, or stepped ***electromagnetic*** field. These systems induce an electrical current (***eddy current***) in the ground that persists after the ***primary field*** is turned off, and measure the change over time of the ***secondary field*** created as the currents ***decay***. See also ***frequency-domain***.

total energy envelope: The sum of the squares of the three ***components*** of the ***time-domain electromagnetic secondary field***. Equivalent to the ***amplitude*** of the secondary field.

transient: Time-varying. Usually used to describe a very short period pulse of ***electromagnetic*** field.

traverse line: A normal geophysical survey line. Normally parallel traverse lines are flown across the property in spacing of 50 m to 500 m, and generally perpendicular to the target geology.

vertical plate: A standard model for electromagnetic geophysical theory. It is usually defined as thin, and ***infinite*** in horizontal dimension and depth extent. (see also ***thin shee***t)

waveform: The shape of the ***electromagnetic pulse*** from a ***time-domain*** electromagnetic transmitter.

window: A discrete portion of a ***gamma-ray spectrum*** or ***time-domain electromagnetic decay***. The continuous energy spectrum or ***full-stream*** data are grouped into windows to reduce the number of samples, and reduce ***noise***.

Version 1.1, March 10, 2003
Greg Hodges,
Chief Geophysicist
Fugro Airborne Surveys, Toronto

Common Symbols and Acronyms

k Magnetic susceptibility
ε Dielectric permittivity
μ, μ_r Magnetic permeability, apparent permeability
ρ, ρ_a Resistivity, apparent resistivity
σ,σ_a Conductivity, apparent conductivity
σt Conductivity thickness
τ Tau, or time constant
Ω.m Ohm-metres, units of resistivity
AGS Airborne gamma ray spectrometry.
CDT Conductivity-depth transform, conductivity-depth imaging (Macnae and Lamontagne, 1987; Wolfgram and Karlik, 1995)
CPI, CPQ Coplanar in-phase, quadrature
CPS Counts per second
CTP Conductivity thickness product
CXI, CXQ Coaxial, in-phase, quadrature
fT femtoteslas, normal unit for measurement of B-Field
EM Electromagnetic
keV kilo electron volts – a measure of gamma-ray energy
MeV mega electron volts – a measure of gamma-ray energy 1MeV = 1000keV
NIA dipole moment: turns x current x Area
nT nano-Tesla, a measure of the strength of a magnetic field
ppm parts per million – a measure of secondary field or noise relative to the primary.
pT/s picoTeslas per second: Units of decay of secondary field, dB/dt
S Siemens – a unit of conductance
x: the horizontal component of an EM field parallel to the direction of flight.
y: the horizontal component of an EM field perpendicular to the direction of flight.
z: the vertical component of an EM field.

References:

Constable, S.C., Parker, R.L., And Constable, C.G., 1987, Occam's inversion: a practical algorithm for generating smooth models from electromagnetic sounding data: Geophysics, 52, 289-300

Huang, H. and Fraser, D.C, 1996. The differential parameter method for muiltifrequency airborne resistivity mapping. Geophysics, 55, 1327-1337

Huang, H. and Palacky, G.J., 1991, Damped least-squares inversion of time-domain airborne EM data based on singular value decomposition: Geophysical Prospecting, v.39, 827-844

Macnae, J. and Lamontagne, Y., 1987, Imaging quasi-layered conductive structures by simple processing of transient electromagnetic data: Geophysics, v52, 4, 545-554.

Sengpiel, K-P. 1988, Approximate inversion of airborne EM data from a multi-layered ground. Geophysical Prospecting, 36, 446-459

Wolfgram, P. and Karlik, G., 1995, Conductivity-depth transform of GEOTEM data: Exploration Geophysics, 26, 179-185.

Yin, C. and Fraser, D.C. (2002), The effect of the electrical anisotropy on the responses of helicopter-borne frequency domain electromagnetic systems, Submitted to *Geophysical Prospecting*